

Article citation info:

Wang E, Wu X, Liu D, Wang S, Shang Y, Artificial neural network supported monotonic stochastic processes for reliability analysis considering multi-uncertainties, *Eksploracja i Niezawodność – Maintenance and Reliability* 2025: 27(3) <http://doi.org/10.17531/ein/197051>

Artificial neural network supported monotonic stochastic processes for reliability analysis considering multi-uncertainties

Indexed by:
 Web of Science Group

Enrui Wang^{a,b}, Xiao Wu^c, Di Liu^{a,b,*}, Shaoping Wang^{a,b}, Yaoxing Shang^{a,b}

^a School of Automation Science and Electrical Engineering, Beihang University, Beijing, 100191, China

^b Tianmushan Laboratory, 311115, China

^c Research Institute of Aero-Engine, Beihang University, Beijing, 100191, China

Highlights


- Process, mean function and parameter uncertainties are considered simultaneously.
- IG and Gamma processes are cooperated with ANN.
- BMA method is introduced to estimate the model parameters and probabilities.

Abstract

Focusing on nonmonotonic degradation processes, we have cooperated artificial neural network (ANN) with Wiener process to utilize its powerful ability on curve fitting. While, the degradation processes of some actual products are determined as monotonic. Furthermore, the process uncertainty issue is also neglected, which is inevitable in engineering practice. Hence, focusing on monotonic degradation dataset, this research introduces ANN-based stochastic process for reliability analysis under multiple uncertainties, including random effects, process uncertainty and mean function uncertainty. The ANN-supported inverse Gaussian and Gamma process models subject to random effects are built. The related parameter estimation and updating methods are also constructed by utilizing moment estimation (ME), Akaike information criterion (AIC) and fully Bayesian inference methods. According to the simulation experiment and actual case study, the proposed method provides higher accuracies on population degradation modeling and monitoring individual degradation prediction.

Keywords

artificial neural network, stochastic process, monotonic degradation, multi-uncertainties, reliability analysis

This is an open access article under the CC BY license (<https://creativecommons.org/licenses/by/4.0/>) 

1. Introduction

Reliability plays a significant role in the design of modern industrial products, and a number of reliability analysis methods have been proposed in the literatures, including the hardware systems and the related software.^{1,2} The reliabilities of the key components are basics for analyzing the system reliability. Namely, the system would have high reliability when the key components are high reliable. Two types of methods have been constructed and applied to estimate the reliabilities of the components in the system for making sure they are reliable

enough during the usage period. The data-driven methods are suitable for the easily monitoring components, such as the power MOSFETs, Li-Ion Battery, reactor protection system, etc.³⁻⁷ Generally, the accuracies of the data-driven methods highly depend on the quality of the degradation data, but it may be difficult to get enough high-quality data for some engineering applications. Hence, the other type of methods, model-based methods, are widely applied. Moreover, the stochastic processes are one kind of the most practical

(*) Corresponding author.

E-mail addresses:

E. Wang (ORCID: 0009-0005-9596-7664) wangenrui@buaa.edu.cn, X. Wu (ORCID: 0009-0009-1176-1052) wx_delta@buaa.edu.cn, D. Liu (ORCID: 0000-0002-8232-4089) liudi54834@buaa.edu.cn, S. Wang (ORCID: 0000-0002-8102-3436) shaopingwang@buaa.edu.cn, Y. Shang syx@buaa.edu.cn.

approaches when applying the model-based methods. The stochastic processes are normally divided into two categories, including the non-monotonic processes and monotonic processes.⁸ According to the previous published researches, the Wiener processes are suitable for the on-monotonic degradation dataset, such as the degradation of the bridge beams due to chloride ion ingress⁹, degradation of LED lamps¹⁰ and degradation of rail tracks¹¹. For some applications, the degradation of the research object is identified as monotonic. Inverse Gaussian (IG) and Gamma processes are commonly used to analyze the degradation datasets with monotonic characteristics.¹² Ye et al. have investigated the IG process as an effective degradation model and proposed several IG process degradation models, including random drift model, random volatility model and random drift-volatility model.¹³ Ye et al. have also employed the IG process to plan the accelerated degradation test.¹⁴ Some similar researches focusing on applying IG process in reliability estimation can also be found in Refs. 15,16. While, the Gamma process may be more suitable for some other applications than the Wiener and IG processes, when estimating the reliability and planning accelerated degradation test.^{17,18} Namely, the process uncertainty issue is inevitable, even though the monotonic degradation datasets are focused in this research. However, the above-mentioned researches neglect the process uncertainty issue. Normally, one specific process is selected before model one degradation dataset.

In other words, when using stochastic process, the degradation processes should be determined to describe the degradation model and estimate the reliability. Some criterions are utilized to select the best fitting model, such as Bayesian information criterion (BIC) and AIC.¹⁹⁻²¹ While, more than one model might be plausible to describe one specific degradation dataset, so selecting one model is not suitable. To handle the process uncertainty issue, several researches have been performed. Liu et al. have applied Bayesian model averaging method (BMA) in accelerated degradation testing analysis.²² The Wiener, IG and Gamma processes are used to analyze the accelerated degradation dataset. The authors argue that the BMA method performs better than the model selection method. Furthermore, we have combined the Gamma and IG processes by using BMA method considering the model uncertainty issue

in monotonic degradation dataset analysis.²³ It is concluded that the IG and Gamma processes are suitable and the BMA method is applicable in monotonic degradation dataset analysis considering the process uncertainty. We have also successfully applied the above method in rotary lip seal degradation modeling and reliability estimation.²⁴ In this paper, the monotonic degradation process is focused, so the Gamma and IG processes are used. Besides, the BMA method is applied considering the powerful ability on process combination and parameter estimation. However, beside the degradation process, the mean function also needs to be determined. Most of the above-mentioned researches focus on the linear degradation processes, while most of industrial products may not linearly degenerate. Namely, besides the process uncertainty issue, the mean function uncertainty issue needs to be discussed further.

A number of researches have been performed to model the nonlinear degradation processes. Peng et al. have constructed a reliability analysis method for the degradation process subject to the time-varying operating missions.²⁵ Based on several IG process models with variable degradation rates, they have also presented Bayesian degradation analysis.²⁶ The constant, monotonic, and S-shaped degradation rates are considered. A Bayesian framework is constructed and verified by several actual case studies to utilize the presented models. Furthermore, considering the multi-phase features of some applications, a number of researches have been performed to model and analyze the multi-phase deteriorating processes.²⁷⁻²⁹ However, the degradation mean function of one specific application may be not within the above known mean functions. Hence, benefiting from the approximation ability of ANN, we have carried out a series of studies to handle the mean function uncertain issue.³⁰ The Wiener process model based on ANN has been proposed. The individual difference and measurement error are taken into account. Both accelerated degradation and life testing datasets are used for the reliability estimation of the products. But, it is a pity that the above-mentioned works only focus on the non-monotonic degradation processes and neglect the process uncertainty issue. Namely, we have cooperated ANN with Wiener process to utilize its powerful ability on curve fitting, but process uncertainty issue is neglected.

The last one factor needs to be determined is the model parameters. Due to the individual difference among the product

population, random effects should be considered in the stochastic process degradation model.^{31,32} Several methods have been presented to handle the above parameter uncertainty issue. For instance, Li et al have cooperated random fuzzy theory with the Wiener process to analyze the accelerated degradation data.³³ To estimate the reliability of the products focusing on small sample conditions, we have also adapted the evidence theory to the Wiener process.³⁴ Beside the above mentioned methods, the Bayesian approaches are the most commonly used kind of parameter estimation and updating methods due to its powerful ability on data and model fusion, as well as the solid theoretical foundation. A number of researches have been performed to utilize Bayesian method in parameters estimation. For instance, Peng et al have presented a Bayesian method to analyze the system reliability with multilevel pass-fail, lifetime and degradation datasets.³⁵ They have also given several Bayesian inference methods to apply the stochastic process models during the degradation analysis.³⁶ Additional similar works can be also found in Refs. 37,38. The related researchers argue that the Bayesian method shows superiority in parameter estimation by fusing data. Hence, the Bayesian method is employed in this paper considering its powerful ability on data and model fusion. However, all the above-mentioned researches neglect the mean function uncertainty issue.

In summary, the process uncertainty, mean function uncertainty and random effects should be considered simultaneously when using stochastic process in engineering practices. Although we have cooperated ANN with Wiener process to utilize its powerful ability on curve fitting, process uncertainty issue is neglected. Namely, only one or two issues are considered in the previously published researches. Hence, to handle the multi-uncertainties issue simultaneously, this paper presents an ANN stochastic process-based reliability analysis approach focusing on monotonic degradation. The new contributions of this research are given below. The process uncertainty, mean function uncertainty and random effects are considered simultaneously. To describe the monotonic degradation processes and handle the mean function uncertainty issue, the IG and Gamma processes are cooperated with ANN, respectively. BMA approach is incorporated to estimate the model parameters and handle the process uncertainty issue.

The remainder of this article is organized as follows. Section

2 illustrates the motivation and methodology. The ANN-supported monotone stochastic processes with random effects are constructed in Section 3. Section 4 and Section 5 present the population reliability modeling and individual reliability prediction methods, respectively. In Section 6, the proposed framework is illustrated. Section 7 verifies the proposed method by actual case studies. Section 8 concludes the paper.

2. Motivation and methodology

Consider a stochastic degradation process $Y(t)$, the initial degradation $Y(0)=0$ and probability is equal to 1. Furthermore, $Y(t)$ has independent increments and the degradation increments $\Delta Y(t)$ can be given by Eq.(1).

$$\Delta Y(t) \sim f(\Delta \Lambda(t) | \theta) \quad (1)$$

where $\Delta Y(t)=Y(t+\Delta t)-Y(t)$ means the degradation increments, Δt means the time increments. $\Delta \Lambda(t)=\Lambda(t+\Delta t)-\Lambda(t)$ indicates the mean function $\Lambda(t)$ increment during time increment Δt . f represents a probability density function (PDF). θ means the corresponding model parameters.

Intuitively, when modeling the degradation process of a specific type of products based on stochastic processes, the following three factors need to be defined. First, the form of the PDF, f , is decided by the applying process. The monotonic degradation processes are focused in this paper, so the Gamma and IG processes are introduced. Second, the mean function $\Lambda(t)$ indicates the degradation law of one specific kind of products and depends on the failure physics of the products. Finally, the model parameters θ are always evaluated based on the measured degradation data. Generally, the model parameters should vary with the different individuals. As a results, the parameter uncertainty issue is inevitable when modeling the degradation of the product population. Furthermore, the process and mean function uncertainty issues are also inevitable, due to lack of the failure theory of the products.

As a result, the process uncertainty, mean function uncertainty and random effects should be considered simultaneously when using stochastic process in engineering practices. Hence, in order to deal with the above uncertainties simultaneously, an ANN supported stochastic process-based reliability analysis method is constructed, as shown in Fig. 1. Λ_{Ga} and $\Delta \Lambda_{Ga}$ indicate the mean function and the corresponding increments of the degradation mean function under Gamma

process. $Ga(\cdot, \cdot)$ denotes the Gamma distribution. θ_{Ga} are the model parameters and θ_{Ga}^H are the corresponding hyper parameters. Λ_{IG} and $\Delta\Lambda_{IG}$ indicate the mean function and the corresponding increments of the degradation mean function under IG process. $IG(\cdot, \cdot)$ represents the IG distribution. θ_{IG} are the model parameters and θ_{IG}^H are the corresponding hyper parameters.

The main idea is as follows. First, the Gamma and IG processes are introduced as candidates to model the monotonic degradation process considering the process uncertainty issue.

Second, inspired by the ANN's powerful ability on the curve fitting, the ANN supported mean function is constructed to handle the uncertain mean function. Third, the ANN-based monotone stochastic processes with random effects are constructed by assuming the model parameters to be randomly distributed, including the IG and Gamma process models. Furthermore, this paper has also built the corresponding parameters estimation method by employing ME, AIC and fully Bayesian inference methods to apply the proposed stochastic processes.

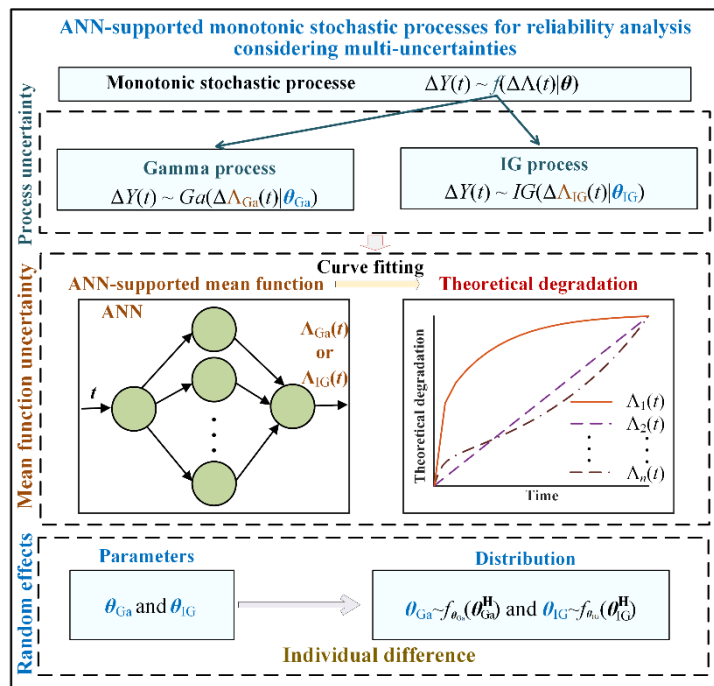


Fig. 1. Schematic of the method.

3. ANN supported monotone stochastic process models with random effects

First, an ANN-supported mean function is proposed, see Section 3.1. Then, the ANN-supported Gamma and IG process models with random effects are constructed based on the mean function, see Section 3.2 and Section 3.3, respectively.

3.1. ANN-supported mean function

The mean function is generally not complicated. Furthermore, using the simple and small ANN can result in small amount of data is enough to train the ANN. Hence, the mean function is described by using a three-layer single input single output (SISO) ANN, as shown in Fig. 2.

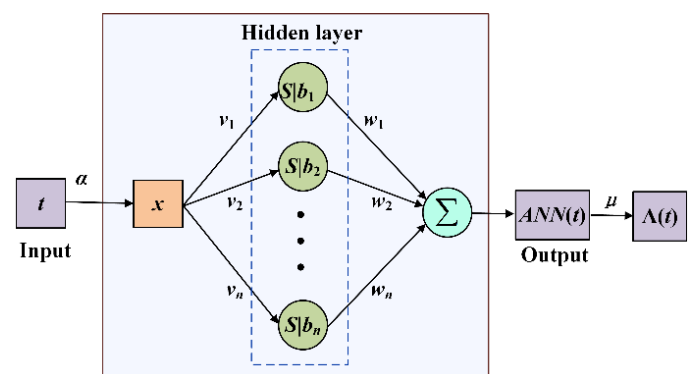


Fig. 2. Schematic of the ANN supported mean function.

Namely, the mean function $\Lambda(t)$ can be approximated as

$$\Lambda(t) = \mu \sum_{k=1}^n w_k S(v_k \alpha t + b_k) \quad (2)$$

where n denotes the neuron size in the hidden layer. μ is used to reflect the changing rate of the function. α is called the shape parameter. v_k and w_k mean the k -th weights of the input and output layers, respectively. b_k means the bias of k -th hidden

neuron. Furthermore, $S(\cdot)$ means the activation function and the sigmoid function is applied. Namely,

$$S(x) = \frac{1}{1+e^{-x}} \quad (3)$$

The parameters, α and μ , are varied with the different individuals. To simplify the expression, the mean function is expressed as

$$\Lambda(t) = \mu ANN(\alpha t) \quad (4)$$

where $ANN(\cdot)$ means the SISO ANN. In the presented work, the ANN is different from the parameters, α and μ , it is independent from the individuals, because it indicates the failure mechanism.

3.2. ANN-supported Gamma process model with random effects

The ANN-supported Gamma process model is constructed on the basis of the above mentioned mean function. For the Gamma process model, the increments are independent and given by Ref. 38.

$$\Delta Y \sim Ga\left(\frac{1}{\lambda_{Ga}} \Delta \Lambda_{Ga}, \lambda_{Ga}\right) \quad (5)$$

where Λ_{Ga} and $\Delta \Lambda_{Ga}$ indicate the mean function and the corresponding increments of the degradation mean function under Gamma process. $Ga(\cdot, \cdot)$ denotes the Gamma distribution and the corresponding PDF is $f_{Ga}(x|a, b) = \frac{1}{\Gamma(a)b^a} x^{a-1} e^{-\frac{x}{b}}$, $x > 0$. Hence, for the above Gamma process model, the degradation mean and variant are $\Delta \Lambda_{Ga}$ and $\lambda_{Ga}^2 \Delta \Lambda_{Ga}$. Furthermore, the PDF of the increment distribution is given by

$$f_{Ga}\left(\Delta y \left| \frac{1}{\lambda_{Ga}} \Delta \Lambda_{Ga}, \lambda_{Ga}\right.\right) = f_{Ga}(\Delta y | \mu_{Ga} \Delta ANN_{Ga}, \lambda_{Ga}) = \frac{1}{\Gamma\left(\frac{1}{\lambda_{Ga}} \mu_{Ga} \Delta ANN_{Ga}\right) \lambda_{Ga}^{\frac{1}{\lambda_{Ga}} \mu_{Ga} \Delta ANN_{Ga}}} \Delta y^{\frac{1}{\lambda_{Ga}} \mu_{Ga} \Delta ANN_{Ga} - 1} e^{-\frac{\Delta y}{\lambda_{Ga}}} \quad (6)$$

where $\Gamma(\cdot)$ indicates the Gamma function, α_{Ga} , μ_{Ga} and λ_{Ga} are the Gamma process model parameters.

The first-passage-time (FPT) distribution is given by

$$f_{Ga}^L(t | ANN_{Ga}, \theta_{Ga}, D) = \frac{d}{dt} \frac{\Gamma\left(\frac{\mu_{Ga} ANN(\alpha_{Ga} t)}{\lambda_{Ga}}, \lambda_{Ga} D\right)}{\Gamma\left(\frac{\mu_{Ga} ANN(\alpha_{Ga} t)}{\lambda_{Ga}}\right)} \quad (7)$$

where $\theta_{Ga} = [\alpha_{Ga}, \mu_{Ga}, \lambda_{Ga}]$ and D means the pre-defined failure threshold.

The reliability function can be derived as

$$R_{Ga}(t | ANN_{Ga}, \theta_{Ga}, D) = 1 - \frac{\Gamma\left(\frac{\mu_{Ga} ANN(\alpha_{Ga} t)}{\lambda_{Ga}}, \frac{D}{\lambda_{Ga}}\right)}{\Gamma(\mu_{Ga} ANN(\alpha_{Ga} t))} \quad (8)$$

Moreover, the random effects are introduced to handle parameter uncertainty issue caused by individual difference when analyzing the population degradation and reliability. Hence, the model parameters are assumed to be randomly distributed with hyper-parameters, as

$$\begin{cases} \mu_{Ga} \sim f_{\mu_{Ga}}(\delta_{\mu_{Ga}}, \gamma_{\mu_{Ga}}) \\ \alpha_{Ga} \sim f_{\alpha_{Ga}}(\delta_{\alpha_{Ga}}, \gamma_{\alpha_{Ga}}) \\ \lambda_{Ga} \sim f_{\lambda_{Ga}}(\delta_{\lambda_{Ga}}, \gamma_{\lambda_{Ga}}) \end{cases} \quad (9)$$

where $f_{\mu_{Ga}}(\cdot, \cdot)$, $f_{\alpha_{Ga}}(\cdot, \cdot)$ and $f_{\lambda_{Ga}}(\cdot, \cdot)$ are the distributions for the model parameters, respectively. $\delta_{\mu_{Ga}}, \gamma_{\mu_{Ga}}, \delta_{\alpha_{Ga}}, \gamma_{\alpha_{Ga}}, \delta_{\lambda_{Ga}}, \gamma_{\lambda_{Ga}}$ and $\gamma_{\mu_{Ga}}$ are the corresponding hyper-parameters. Furthermore, $\theta_{Ga} = [\mu_{Ga}, \alpha_{Ga}, \lambda_{Ga}]$ are the model parameters and $\theta_{Ga}^H = [\delta_{\mu_{Ga}}, \gamma_{\mu_{Ga}}, \delta_{\alpha_{Ga}}, \gamma_{\alpha_{Ga}}, \delta_{\lambda_{Ga}}, \gamma_{\lambda_{Ga}}]$ are the corresponding hyper-parameters. Similar as Ref. 30, Gamma, lognormal and Gaussian distributions are introduced as the candidate distributions for the model parameters. The corresponding PDFs are shown in Eq.(10). Furthermore, the best fitting distributions can be selected based on AIC for each model parameters.

The PDFs of lognormal, Gaussian and Gamma distributions are given by

$$\begin{cases} f_{LN}(x|\delta, \gamma) = \begin{cases} \frac{1}{x\gamma\sqrt{2\pi}} e^{-\frac{(\ln x - \delta)^2}{2\gamma^2}} & 0 < x \\ 0 & \text{other} \end{cases} \\ f_N(y|\delta, \gamma^2) = \frac{1}{\gamma\sqrt{2\pi}} \exp\left[-\frac{(y-\delta)^2}{2\gamma^2}\right] \\ f_{Ga}(x|\delta, \gamma) = \frac{x^{\delta-1}}{\Gamma(\delta)\gamma^\delta} \exp\left(-\frac{x}{\gamma}\right) \end{cases} \quad (10)$$

3.3. ANN-supported IG process model with random effects

The ANN-supported IG process model is also constructed using the above mentioned mean function. For the IG process model, the increments are independent and given by Ref. 38.

$$\Delta Y \sim IG(\Delta \Lambda_{IG}, \Delta \Lambda_{IG}^2 / \lambda_{IG}) \quad (11)$$

where Λ_{IG} and $\Delta \Lambda_{IG}$ indicate the mean function and the corresponding increments of the degradation mean function under IG process. $IG(\cdot, \cdot)$ represents the IG distribution and the corresponding PDF is $f_{IG}(x|a, b) = \left(\frac{b}{2\pi x^3}\right)^{0.5} \exp\left[-\frac{b(x-a)^2}{2a^2 x}\right]$, $x > 0$. Hence, for the above IG process model, the degradation mean and variance are $\Delta \Lambda_{IG}$ and $\Delta \Lambda_{IG} / \lambda_{IG}$. Furthermore, the PDF of the increment distribution is given by

$$f_{IG}(\Delta y|\Delta\Lambda_{IG}, \lambda_{IG}) = f_{IG}(\Delta y|\mu_{IG}\Delta ANN_{IG}, \lambda_{IG}) = \left(\frac{\lambda_{IG}\mu_{IG}^2\Delta ANN_{IG}^2}{2\pi\Delta y^3}\right)^{0.5} \exp\left[-\frac{\lambda_{IG}\mu_{IG}\Delta ANN_{IG}(\Delta y-\mu_{IG}\Delta ANN_{IG})^2}{2\mu_{IG}^2\Delta ANN_{IG}^2\Delta y}\right] \quad (12)$$

The distribution of FPT is given by

$$f_{IG}^L(t|ANN_{IG}, \theta_{IG}, D) = 2\sqrt{\frac{\lambda_{IG}}{D}}\phi\left[\sqrt{\frac{\lambda_{IG}}{D}}(\mu_{IG}ANN_{IG}(\alpha_{IG}t) - D)\right] - 2\lambda_{IG}\exp(2\lambda_{IG}\mu_{IG}ANN_{IG}(\alpha_{IG}t))\Phi\left[-\sqrt{\frac{\lambda_{IG}}{D}}(\mu_{IG}ANN_{IG}(\alpha_{IG}t) + D)\right] \quad (13)$$

where $\Phi(\cdot)$ and $\phi(\cdot)$ mean the cumulative probability function (CDF) and PDF of the standard normal distribution. Moreover, $\theta_{IG} = [\alpha_{IG}, \mu_{IG}, \lambda_{IG}]$.

The corresponding reliability function can be calculated as

$$R_{IG}(t|ANN_{IG}, \theta_{IG}, D) = 1 - \Phi\left[\sqrt{\frac{\lambda_{IG}}{D}}(\mu_{IG}ANN_{IG}(\alpha_{IG}t) - D)\right] + \exp(2\lambda_{IG}\mu_{IG}ANN_{IG}(\alpha_{IG}t))\Phi\left[-\sqrt{\frac{\lambda_{IG}}{D}}(\mu_{IG}ANN_{IG}(\alpha_{IG}t) - D)\right] \quad (14)$$

As discussed in Section 3.2, assuming the model parameters to be randomly distributed, as

$$\begin{cases} \mu_{IG} \sim f_{\mu_{IG}}(\delta_{\mu_{IG}}, \gamma_{\mu_{IG}}) \\ \alpha_{IG} \sim f_{\alpha_{IG}}(\delta_{\alpha_{IG}}, \gamma_{\alpha_{IG}}) \\ \lambda_{IG} \sim f_{\lambda_{IG}}(\delta_{\lambda_{IG}}, \gamma_{\lambda_{IG}}) \end{cases} \quad (15)$$

$$L_{Ga}(Y_{1:n_d}|T_{1:n_d}, \theta_{Ga1:n_d}, ANN_{Ga}) = \prod_{i=1}^{n_d} \prod_{j=1}^{N_i-1} f_{Ga}(\Delta y_{ij}|\mu_{Gai}\Delta ANN_{Gaij}, \lambda_{Gai}) = \prod_{i=1}^{n_d} \prod_{j=1}^{N_i-1} \frac{1}{\Gamma\left(\frac{1}{\lambda_{Gai}}\mu_{Gai}\Delta ANN_{Gaij}\right)\lambda_{Gai}^{\frac{1}{\lambda_{Gai}}\mu_{Gai}\Delta ANN_{Gaij}}} \Delta y_{ij}^{\frac{1}{\lambda_{Gai}}\mu_{Gai}\Delta ANN_{Gaij}-1} e^{-\frac{\Delta y_{ij}}{\lambda_{Gai}}} \quad (18)$$

where $\theta_{Ga1:n_d} = [\alpha_{Ga1:n_d}; \mu_{Ga1:n_d}; \lambda_{Ga1:n_d}]$, $\alpha_{Ga1:n_d} = [a_{Ga1}, a_{Ga2}, \dots, a_{Gan_d}]$, $\mu_{Ga1:n_d} = [\mu_{Ga1}, \mu_{Ga2}, \dots, \mu_{Gan_d}]$ and $\lambda_{Ga1:n_d} = [\lambda_{Ga1}, \lambda_{Ga2}, \dots, \lambda_{Gan_d}]$ are the model parameters for different samples. ΔANN_{Gaij} means the increments of i -th sample between $(j-1)$ -th to j -th observation time. Δy_{ij} means the degradation increments of i -th sample between $(j-1)$ -th to j -th observations.

The related minus log-likelihood function can be written as

$$l_{Ga}(Y_{1:n_d}|T_{1:n_d}, \theta_{Ga1:n_d}, ANN_{Ga}) = -\ln L_{Ga}(Y_{1:n_d}|T_{1:n_d}, \theta_{Ga1:n_d}, ANN_{Ga}) \quad (19)$$

A larger value of likelihood means the better fitting performance of the model to the dataset. In other words, the corresponding minus log-likelihood function is smaller, the

where $f_{\mu_{IG}}(\cdot, \cdot)$, $f_{\alpha_{IG}}(\cdot, \cdot)$ and $f_{\lambda_{IG}}(\cdot, \cdot)$ are the distributions for the model parameters. $\theta_{IG} = [\mu_{IG}, \alpha_{IG}, \lambda_{IG}]$ are the model parameters and $\theta_{IG}^H = [\delta_{\mu_{IG}}, \gamma_{\mu_{IG}}, \delta_{\alpha_{IG}}, \gamma_{\alpha_{IG}}, \delta_{\lambda_{IG}}, \gamma_{\lambda_{IG}}]$ are the corresponding hyper parameters.

4. Population degradation modeling

The degradation dataset includes the degradation observations $Y_{1:n_d} = [Y_1, Y_2, \dots, Y_{n_d}]$ and the corresponding measurement time $T_{1:n_d} = [T_1, T_2, \dots, T_{n_d}]$, where n_d means the sample size. The degradation observations of i -th sample Y_i and the corresponding time T_i are given by

$$Y_i = [y_{i1}, y_{i2}, \dots, y_{iN_i}] \quad (16)$$

$$T_i = [t_{i1}, t_{i2}, \dots, t_{iN_i}] \quad (17)$$

where y_{ij} and t_{ij} are j -th observation and the corresponding time of i -th sample, the observation size of i -th sample is denoted as N_i .

4.1. Training approach of ANN-supported mean function

4.1.1. Gamma process model

Given the degradation dataset, for the Gamma process model, the related log-likelihood function is given by

goodness-of-fit is better. Hence, based on the likelihood function, the loss function is defined as

$$E_{Ga} = l_{Ga}(Y_{1:n_d}|T_{1:n_d}, \theta_{Ga1:n_d}, ANN_{Ga}) \quad (20)$$

Furthermore, the mean function and process parameters should be monotonic increasing and nonnegative considering their physical meanings. Hence, the ANN supported Gamma process based model can be trained by minimizing the loss function with inequality constraints, as shown in Eq.(21).

$$\begin{aligned} \min E_{Ga} &= l_{Ga}(Y_{1:n_d}|T_{1:n_d}, \theta_{Ga1:n_d}, ANN_{Ga}) \text{ s.t. } \frac{dANN_{Ga}(t)}{dt} > 0 \\ &\quad \forall i, \mu_{Gai} > 0, \alpha_{Gai} > 0, \lambda_{Gai} > 0 \end{aligned} \quad (21)$$

Genetic algorithm is introduced to train the ANN supported mean function and handled by utilizing *ga* function in Matlab software. The main configuration parameters for the presented

simulation and case studies are: the constraint tolerance is set to be 0.001, the crossover fraction is set to be 0.8, the population size is set to be 200, the function tolerance is set to be 0.000001. The model parameters' training results are expressed as $\tilde{\alpha}_{Ga1:n_d}$, $\tilde{\mu}_{Ga1:n_d}$ and $\tilde{\lambda}_{Ga1:n_d}$. \overline{ANN}_{Ga} means the trained ANN of the Gamma process model. $\tilde{\theta}_{Gai} = [\tilde{\mu}_{Gai}, \tilde{\alpha}_{Gai}, \tilde{\lambda}_{Gai}]$ and $\tilde{\theta}_{Ga1:n_d} =$

$$L_{IG}(Y_{1:n_d}|T_{1:n_d}, \theta_{IG1:n_d}, ANN_{IG}) = \prod_{i=1}^{n_d} \prod_{j=1}^{N_i-1} f_{IG}(\Delta y_{ij} | \mu_{IGi} \Delta ANN_{IGij}, \lambda_{IGi}) = \prod_{i=1}^{n_d} \prod_{j=1}^{N_i-1} \left(\frac{\lambda_{IGi} \mu_{IGi}^2 \Delta ANN_{IGij}^2}{2\pi \Delta y_{ij}^3} \right)^{0.5} \exp \left[-\frac{\lambda_{IGi} \mu_{IGi} \Delta ANN_{IGij} (\Delta y_{ij} - \mu_{IGi} \Delta ANN_{IGij})^2}{2\mu_{IGi}^2 \Delta ANN_{IGij}^2 \Delta y_{ij}} \right] \quad (22)$$

where $\theta_{IG1:n_d} = [\alpha_{IG1:n_d}; \mu_{IG1:n_d}; \lambda_{IG1:n_d}]$, $\alpha_{IG1:n_d} = [a_{IG1}, a_{IG2}, \dots, a_{IGn_d}]$, $\mu_{IG1:n_d} = [\mu_{IG1}, \mu_{IG2}, \dots, \mu_{IGn_d}]$ and $\lambda_{IG1:n_d} = [\lambda_{IG1}, \lambda_{IG2}, \dots, \lambda_{IGn_d}]$ are the model parameters for different samples. ΔANN_{IGij} means the increments of i -th sample between $(j-1)$ -th to j -th observation time.

The related minus log-likelihood function can be written as $l_{IG}(Y_{1:n_d}|T_{1:n_d}, \theta_{IG1:n_d}, ANN_{IG}) = -\ln L_{IG}(Y_{1:n_d}|T_{1:n_d}, \theta_{IG1:n_d}, ANN_{IG})$ (23)

Similarly, a larger value of likelihood means the better fitting performance of the model to the dataset. Furthermore, the model parameters should be nonnegative and the mean function should increase in a monotonical manner. Hence, the IG process model can be trained by Eq.(24).

$$\min E_{IG} = l_{IG}(Y_{1:n_d}|T_{1:n_d}, \theta_{IG1:n_d}, ANN_{IG}) \text{ s.t. } \frac{dANN_{IG}(t)}{dt} > 0 \quad \forall i, \mu_{IGi} > 0, \alpha_{IGi} > 0, \lambda_{IGi} > 0 \quad (24)$$

Similarly, Eq.(24) is handled by genetic algorithm. The main configuration parameters for the presented simulation and case studies are as Section 4.1.1. The model parameters' training results are expressed as $\tilde{\theta}_{IG1:n_d}$, $\tilde{\alpha}_{IG1:n_d}$, $\tilde{\mu}_{IG1:n_d}$ and $\tilde{\lambda}_{IG1:n_d}$.

$$\begin{cases} L_{Gai}(Y_i|T_i, \tilde{\theta}_{Gai}, \overline{ANN}_{Ga}) = \prod_{j=1}^{N_i-1} \frac{1}{\Gamma\left(\frac{1}{\lambda_{Gai}} \mu_{Gai} \Delta ANN_{Gaij}\right) \lambda_{Gai}^{\frac{1}{\lambda_{Gai}} \mu_{Gai} \Delta ANN_{Gaij}}} \Delta y_{ij}^{\frac{1}{\lambda_{Gai}} \mu_{Gai} \Delta ANN_{Gaij} - 1} e^{-\frac{\Delta y_{ij}}{\lambda_{Gai}}} \\ L_{IGi}(Y_i|T_i, \tilde{\theta}_{IGi}, \overline{ANN}_{IG}) = \prod_{j=1}^{N_i-1} \left(\frac{\lambda_{IGi} \mu_{IGi}^2 \Delta ANN_{IGij}^2}{2\pi \Delta y_{ij}^3} \right)^{0.5} \exp \left[-\frac{\lambda_{IGi} \mu_{IGi} \Delta ANN_{IGij} (\Delta y_{ij} - \mu_{IGi} \Delta ANN_{IGij})^2}{2\mu_{IGi}^2 \Delta ANN_{IGij}^2 \Delta y_{ij}} \right] \end{cases} \quad (26)$$

Furthermore, concerning the random effects of the model probabilities, the probabilities are also assumed to be randomly distributed, as

$$\begin{cases} p_{Ga} \sim f_{p_{Ga}}(\delta_{p_{Ga}}, \gamma_{p_{Ga}}) \\ p_{IG} = 1 - p_{Ga} \end{cases} \quad (27)$$

where $f_{p_{Ga}}(\cdot, \cdot)$ indicates the PDF of one of the candidate

$[\tilde{\theta}_{Ga1}; \tilde{\theta}_{Ga2}; \dots; \tilde{\theta}_{Gan_d}]$.

4.1.2. IG process model

Given the degradation dataset, for the IG process model, the related log-likelihood function is given by

\overline{ANN}_{IG} means the trained ANN of the Gamma process model. $\tilde{\theta}_{IGi} = [\tilde{\mu}_{IGi}, \tilde{\alpha}_{IGi}, \tilde{\lambda}_{IGi}]$ and $\tilde{\theta}_{IG1:n_d} = [\tilde{\theta}_{IG1}; \tilde{\theta}_{IG2}; \dots; \tilde{\theta}_{IGn_d}]$.

4.2 Model probabilities

According to Bayesian inference, the model probabilities p_{Gai} and p_{IGi} for i -th sample can be calculated as

$$\begin{cases} p_{Gai} = P(M_{Gai}|Y_i, T_i, \tilde{\theta}_{Gai}, \tilde{\theta}_{IGi}, \overline{ANN}_{Ga}, \overline{ANN}_{IG}) \\ = \frac{\pi(M_{Gai}) L_{Gai}(Y_i|T_i, \tilde{\theta}_{Gai}, \overline{ANN}_{Ga})}{\pi(M_{IGi}) L_{IGi}(Y_i|T_i, \tilde{\theta}_{IGi}, \overline{ANN}_{IG}) + \pi(M_{Gai}) L_{Gai}(Y_i|T_i, \tilde{\theta}_{Gai}, \overline{ANN}_{Ga})} \\ p_{IGi} = P(M_{IGi}|Y_i, T_i, \tilde{\theta}_{Gai}, \tilde{\theta}_{IGi}, \overline{ANN}_{Ga}, \overline{ANN}_{IG}) \\ = \frac{\pi(M_{IGi}) L_{IGi}(Y_i|T_i, \tilde{\theta}_{IGi}, \overline{ANN}_{IG})}{\pi(M_{IGi}) L_{IGi}(Y_i|T_i, \tilde{\theta}_{IGi}, \overline{ANN}_{IG}) + \pi(M_{Gai}) L_{Gai}(Y_i|T_i, \tilde{\theta}_{Gai}, \overline{ANN}_{Ga})} \end{cases} \quad (25)$$

where $P(M_{Gai}|Y_i, T_i, \tilde{\theta}_{Gai}, \tilde{\theta}_{IGi}, \overline{ANN}_{Ga}, \overline{ANN}_{IG})$ and $P(M_{IGi}|Y_i, T_i, \tilde{\theta}_{Gai}, \tilde{\theta}_{IGi}, \overline{ANN}_{Ga}, \overline{ANN}_{IG})$ are the posterior probabilities of the candidate models for i -th sample. $\pi(M_{Gai})$ and $\pi(M_{IGi})$ are the prior probabilities of the candidate models. Moreover, the non-informative prior is applied here, namely $\pi(M_{Gai}) = \pi(M_{IGi}) = 0.5$, for $i=1, 2, \dots, n_d$. $L_{IGi}(Y_i|T_i, \tilde{\theta}_{IGi}, \overline{ANN}_{IG})$ and $L_{Gai}(Y_i|T_i, \tilde{\theta}_{Gai}, \overline{ANN}_{Ga})$ are the likelihood function of the candidate models for i -th sample, when the ANN are \overline{ANN}_{IG} and \overline{ANN}_{Ga} , as well as the model parameters are $\tilde{\theta}_{IGi}$ and $\tilde{\theta}_{Gai}$, as given by

distributions. $\delta_{p_{Ga}}$ and $\gamma_{p_{Ga}}$ are the corresponding hyperparameters.

4.3. Process parameters distributions and population evaluation

In the presented work, the random effects caused by

nonhomogeneous within the product population are considered, so the model parameters are assumed to satisfy the random distribution. The Gamma, lognormal and Gaussian distributions are considered as the candidate distributions. The ME method is used. According to our previously published research, Ref. 30, the hyper-parameters' ME results of the candidate distributions are given as follows.

The ME estimating results for the Gamma distribution are given by

$$\begin{cases} \bar{\delta}_\chi = \frac{(\sum_{i=1}^{n_d} \tilde{\chi}_i)^2}{n_d \sum_{i=1}^{n_d} (\tilde{\chi}_i - \frac{1}{n_d} \sum_{i=1}^{n_d} \tilde{\chi}_i)^2} \\ \bar{\gamma}_\chi = \frac{\sum_{i=1}^{n_d} (\tilde{\chi}_i - \frac{1}{n_d} \sum_{i=1}^{n_d} \tilde{\chi}_i)^2}{\sum_{i=1}^{n_d} \tilde{\chi}_i} \end{cases} \quad (28)$$

where $\tilde{\chi}_i$ means the training result of one of the model parameters for i -th sample, such as $\tilde{\alpha}_{\text{Ga}i}$, $\tilde{\mu}_{\text{Ga}i}$, $\tilde{\lambda}_{\text{Ga}i}$, $\tilde{\alpha}_{\text{IG}i}$, $\tilde{\mu}_{\text{IG}i}$ or $\tilde{\lambda}_{\text{IG}i}$. $\bar{\delta}_\chi$ and $\bar{\gamma}_\chi$ indicate the corresponding hyper-parameters' ME estimating results.

The ME estimating results for the lognormal distribution are given by

$$\begin{cases} \bar{\delta}_\chi = \frac{1}{n_d} \sum_{i=1}^{n_d} \ln(\tilde{\chi}_i) \\ \bar{\gamma}_\chi = \sqrt{\frac{1}{n_d} \sum_{i=1}^{n_d} (\ln(\tilde{\chi}_i) - \frac{1}{n_d} \sum_{i=1}^{n_d} \ln(\tilde{\chi}_i))^2} \end{cases} \quad (29)$$

The ME estimating results for the Gaussian distribution are given by

$$\begin{cases} \bar{\delta}_\chi = \frac{1}{n_d} \sum_{i=1}^{n_d} \chi_i \\ \bar{\gamma}_\chi = \sqrt{\frac{1}{n_d} \sum_{i=1}^{n_d} (\chi_i - \frac{1}{n_d} \sum_{i=1}^{n_d} \chi_i)^2} \end{cases} \quad (30)$$

$$R_p(t | \overline{ANN}_{\text{Ga}}, \overline{ANN}_{\text{IG}}, \theta_{\text{Ga}}, \theta_{\text{IG}}, D) = \int_{p_{\text{Ga}}} \int_{\theta_{\text{Ga}}} \int_{\theta_{\text{IG}}} f_{p_a}(\bar{\delta}_{p_a}, \bar{\gamma}_{p_a}) \left[p_{\text{Ga}} f_{\bar{\theta}_{\text{Ga}}}(\bar{\delta}_{\theta_{\text{Ga}}}, \bar{\gamma}_{\theta_{\text{Ga}}}) R_{\text{Ga}}(t | \overline{ANN}_{\text{Ga}}, \theta_{\text{Ga}}, D) + (1 - p_{\text{Ga}}) f_{\bar{\theta}_{\text{IG}}}(\bar{\delta}_{\theta_{\text{IG}}}, \bar{\gamma}_{\theta_{\text{IG}}}) R_{\text{IG}}(t | \overline{ANN}_{\text{IG}}, \theta_{\text{IG}}, D) \right] d\theta_{\text{IG}} d\theta_{\text{Ga}} dp_{\text{Ga}} \quad (33)$$

$$f_p^L(t | \overline{ANN}_{\text{Ga}}, \overline{ANN}_{\text{IG}}, \theta_{\text{Ga}}, \theta_{\text{IG}}, D) = \int_{p_{\text{Ga}}} \int_{\theta_{\text{Ga}}} \int_{\theta_{\text{IG}}} f_{p_a}(\bar{\delta}_{p_a}, \bar{\gamma}_{p_a}) \left[p_{\text{Ga}} f_{\bar{\theta}_{\text{Ga}}}(\bar{\delta}_{\theta_{\text{Ga}}}, \bar{\gamma}_{\theta_{\text{Ga}}}) f_{\text{Ga}}^L(t | \overline{ANN}_{\text{Ga}}, \theta_{\text{Ga}}, D) + (1 - p_{\text{Ga}}) f_{\bar{\theta}_{\text{IG}}}(\bar{\delta}_{\theta_{\text{IG}}}, \bar{\gamma}_{\theta_{\text{IG}}}) f_{\text{IG}}^L(t | \overline{ANN}_{\text{IG}}, \theta_{\text{IG}}, D) \right] d\theta_{\text{IG}} d\theta_{\text{Ga}} dp_{\text{Ga}} \quad (34)$$

5. Individual degradation prediction

The measured degradation and time of the monitoring individual can be express as

$$Y = [y_1, y_2, \dots, y_N] \quad (35)$$

$$T = [t_1, t_2, \dots, t_N] \quad (36)$$

where y_j and t_j are the j -th measured degradation and the corresponding measurement time of the monitoring individual. N is the measurement size of the monitoring individual.

The model parameters' best fitting distributions are determined based on AIC. The AIC values $AIC = 2k - l(\bar{\delta}_\chi, \bar{\gamma}_\chi)$, where k means the parameter sizes of the candidate distributions, $\bar{\delta}_\chi, \bar{\gamma}_\chi$ means the hyper-parameters' ME approximation results, and $l(\bar{\delta}_\chi, \bar{\gamma}_\chi)$ is the related log-likelihood.²⁰ Note that a small AIC value represents means better goodness-of-fit, so the distributions with the minimum AIC values are selected.

Moreover, the determined model parameter distributions are expressed as

$$\begin{cases} \mu_{\text{Ga}} \sim f_{\bar{\mu}_{\text{Ga}}}(\bar{\delta}_{\mu_{\text{Ga}}}, \bar{\gamma}_{\mu_{\text{Ga}}}), \alpha_{\text{Ga}} \sim f_{\bar{\alpha}_{\text{Ga}}}(\bar{\delta}_{\alpha_{\text{Ga}}}, \bar{\gamma}_{\alpha_{\text{Ga}}}), \lambda_{\text{Ga}} \sim f_{\bar{\lambda}_{\text{Ga}}}(\bar{\delta}_{\lambda_{\text{Ga}}}, \bar{\gamma}_{\lambda_{\text{Ga}}}) \\ \mu_{\text{IG}} \sim f_{\bar{\mu}_{\text{IG}}}(\bar{\delta}_{\mu_{\text{IG}}}, \bar{\gamma}_{\mu_{\text{IG}}}), \alpha_{\text{IG}} \sim f_{\bar{\alpha}_{\text{IG}}}(\bar{\delta}_{\alpha_{\text{IG}}}, \bar{\gamma}_{\alpha_{\text{IG}}}), \lambda_{\text{IG}} \sim f_{\bar{\lambda}_{\text{IG}}}(\bar{\delta}_{\lambda_{\text{IG}}}, \bar{\gamma}_{\lambda_{\text{IG}}}) \\ p_a \sim f_{\bar{p}_a}(\bar{\delta}_{p_a}, \bar{\gamma}_{p_a}), p_{\text{IG}} = 1 - p_{\text{Ga}} \end{cases} \quad (31)$$

The model parameters' distributions are s -independent, so the corresponding joint distributions are given by

$$\begin{cases} f_{\bar{\theta}_{\text{Ga}}}(\bar{\theta}_{\text{Ga}}^H) = f_{\bar{\mu}_{\text{Ga}}}(\bar{\delta}_{\mu_{\text{Ga}}}, \bar{\gamma}_{\mu_{\text{Ga}}}) f_{\bar{\alpha}_{\text{Ga}}}(\bar{\delta}_{\alpha_{\text{Ga}}}, \bar{\gamma}_{\alpha_{\text{Ga}}}) f_{\bar{\lambda}_{\text{Ga}}}(\bar{\delta}_{\lambda_{\text{Ga}}}, \bar{\gamma}_{\lambda_{\text{Ga}}}) \\ f_{\bar{\theta}_{\text{IG}}}(\bar{\theta}_{\text{IG}}^H) = f_{\bar{\mu}_{\text{IG}}}(\bar{\delta}_{\mu_{\text{IG}}}, \bar{\gamma}_{\mu_{\text{IG}}}) f_{\bar{\alpha}_{\text{IG}}}(\bar{\delta}_{\alpha_{\text{IG}}}, \bar{\gamma}_{\alpha_{\text{IG}}}) f_{\bar{\lambda}_{\text{IG}}}(\bar{\delta}_{\lambda_{\text{IG}}}, \bar{\gamma}_{\lambda_{\text{IG}}}) \end{cases} \quad (32)$$

where $\bar{\theta}_{\text{Ga}}^H = [\bar{\delta}_{\mu_{\text{Ga}}}, \bar{\gamma}_{\mu_{\text{Ga}}}, \bar{\delta}_{\alpha_{\text{Ga}}}, \bar{\gamma}_{\alpha_{\text{Ga}}}, \bar{\delta}_{\lambda_{\text{Ga}}}, \bar{\gamma}_{\lambda_{\text{Ga}}}]$ and $\bar{\theta}_{\text{IG}}^H = [\bar{\delta}_{\mu_{\text{IG}}}, \bar{\gamma}_{\mu_{\text{IG}}}, \bar{\delta}_{\alpha_{\text{IG}}}, \bar{\gamma}_{\alpha_{\text{IG}}}, \bar{\delta}_{\lambda_{\text{IG}}}, \bar{\gamma}_{\lambda_{\text{IG}}}]$.

Finally, the reliability function and FPT distribution of the product population are given by

5.1. Model parameters and probabilities priors

To estimate the model probabilities and parameters of the monitoring individual, the fully Bayesian inference approach is introduced. The priors of the model probabilities and parameters are set according to the estimating results of the model parameter distributions at population degradation modeling stage. Namely,

$$\begin{cases} \pi(\theta_{Ga}) \sim f_{\bar{\theta}_{Ga}}(\bar{\theta}_{Ga}^H) \\ \pi(\theta_{IG}) \sim f_{\bar{\theta}_{IG}}(\bar{\theta}_{IG}^H) \\ \pi(p_a) \sim f_{p_a}(\bar{\delta}_p, \bar{\gamma}_{p_a}), p_{IG} = 1 - p_{Ga} \end{cases} \quad (37)$$

5.2. Posterior of the model probabilities and parameters

According to the fully Bayesian inference method, the posterior distribution of the model probabilities and parameters is derived as

$$p(\theta_{Ga}, \theta_{IG}, p_{Ga} | Y, T) = \frac{\pi(\theta_{Ga})\pi(p_{Ga})p_{Ga}L_{Ga}(Y|T, \theta_{Ga}, \overline{ANN}_{Ga}) + \pi(\theta_{IG})\pi(p_{IG})L_{IG}(Y|T, \theta_{IG}, \overline{ANN}_{IG})}{\int p_a \int \theta_{IG} \int \theta_{Ga} + \pi(\theta_{IG})\pi(p_{IG})L_{IG}(Y|T, \theta_{IG}, \overline{ANN}_{IG}) d\theta_{Ga} d\theta_{IG} dp_a} \quad (38)$$

The posterior distribution can be calculated by Eq. (39). Normally, the posterior distributions' mean values are employed to estimate the model parameters.

$$p(\theta_{Ga}, \theta_{IG}, p_{Ga} | Y, T) \propto \pi(\theta_{Ga})\pi(p_{Ga})p_{Ga}L_{Ga}(Y|T, \theta_{Ga}, \overline{ANN}_{Ga}) + \pi(\theta_{IG})\pi(p_{IG})L_{IG}(Y|T, \theta_{IG}, \overline{ANN}_{IG}) \quad (39)$$

where

$$\begin{cases} L_{Ga}(Y|T, \bar{\theta}_{Ga}, \overline{ANN}_{Ga}) = \prod_{j=1}^{N-1} \frac{1}{\Gamma(\frac{1}{\lambda_{Ga}}\mu_{Ga}\Delta ANN_{Gaj})\lambda_{Ga}^{\frac{1}{\lambda_{Ga}}\mu_{Ga}\Delta ANN_{Gaj}}} \Delta y_j^{\frac{1}{\lambda_{Ga}}\mu_{Ga}\Delta ANN_{Gaj}-1} e^{-\frac{\Delta y_j}{\lambda_{Ga}}} \\ L_{IG}(Y|T, \bar{\theta}_{IG}, \overline{ANN}_{IG}) = \prod_{j=1}^{N-1} \left(\frac{\lambda_{IG}\mu_{IG}^2 \Delta ANN_{IGj}^2}{2\pi\Delta y_j^3} \right)^{0.5} \exp \left[-\frac{\lambda_{IG}\mu_{IG}\Delta ANN_{IGj}(\Delta y_j - \mu_{IG}\Delta ANN_{IGj})^2}{2\mu_{IG}^2 \Delta ANN_{IGj}^2 \Delta y_j} \right] \end{cases} \quad (40)$$

where Δy_j means the degradation increments between $(j-1)$ -th to j -th observations of the monitoring individual. ΔANN_{IGj} and ΔANN_{Ga_j} are the corresponding ANN function increments. The $\hat{\theta}_{Ga}$, $\hat{\theta}_{IG}$ and \hat{p}_{Ga} means the inferred model parameters and probabilities.

Finally, for the monitoring individual, the reliability function and FPT distribution are given by

$$R_I(t | \overline{ANN}_{Ga}, \overline{ANN}_{IG}, \hat{\theta}_{Ga}, \hat{\theta}_{IG}, \hat{p}_{Ga}, D) = \hat{p}_{Ga} R_{Ga}(t | \overline{ANN}_{Ga}, \hat{\theta}_{Ga}, D) + (1 - \hat{p}_{Ga}) R_{IG}(t | \overline{ANN}_{IG}, \hat{\theta}_{IG}, D) \quad (41)$$

$$f_I^L(t | \overline{ANN}_{Ga}, \overline{ANN}_{IG}, \hat{\theta}_{Ga}, \hat{\theta}_{IG}, \hat{p}_{Ga}, D) = \hat{p}_{Ga} f_{Ga}^L(t | \overline{ANN}_{Ga}, \hat{\theta}_{Ga}, D) + (1 - \hat{p}_{Ga}) f_{IG}^L(t | \overline{ANN}_{IG}, \hat{\theta}_{IG}, D) \quad (42)$$

6. The proposed framework

Fig. 3, indicates the flowchart of the presented framework.

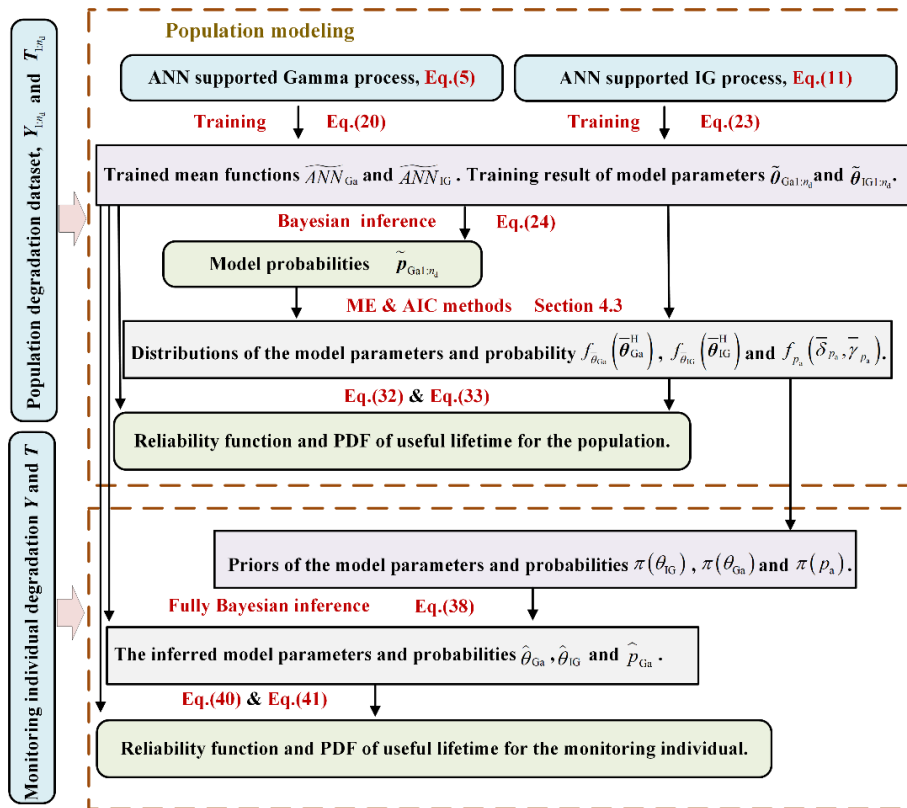


Fig. 3. The flowchart of the presented framework.

Three steps are required when analyzing the population reliability by applying the proposed method. First, the Gamma and IG process models are trained by maximizing the likelihood, see Section 4.1. Second, the model probabilities are evaluated by Bayesian inference method, see Section 4.2. Third, the distributions of model parameters and probabilities are set by applying ME and AIC methods, see Section 4.3. Finally, the population degradation and reliability are modeled by the proposed stochastic process model, Eq.(33) and Eq.(34).

To predict the reliability and life of the monitoring individual in real time, three more steps need to be carried out. First, based on the estimated model parameter distributions at population degradation modeling stage, the priors of the model probabilities and parameters can be determined, see Section 5.1. Then, based on the fully Bayesian inference method, the posterior distributions of model probabilities and parameters for the monitoring individual are obtained, see Section 5.2. Finally, the remaining useful life (RUL) and reliability of the monitoring individual are predicted by the proposed stochastic process model, Eq.(41) and Eq.(42).

Moreover, Algorithm 1 shows the algorithm of the presented framework in detail.

Algorithm 1

Algorithm of the presented framework.

Population reliability analysis

Set the hidden layer neuron size of the ANN.

Train the ANN-supported Gamma and IG process models, Eq.(21) and Eq.(24).

Fix the trained ANNs, including \widehat{ANN}_{Ga} and \widehat{ANN}_{IG} .

Estimate the model probabilities for each degradation samples, Eq.(25).

Calculate the ME results of the hyper-parameters under different candidate distributions, Eq.(28)-Eq.(30).

Select the best fitting distributions for the model parameters and probabilities by AIC.

Infer the population reliability and life distribution, Eq.(33) and Eq.(34).

Individual reliability prediction

Set the model probabilities' and parameters' priors, Eq.(37).

Calculate the model probabilities' and parameters' posterior distributions, Eq.(39).

Infer the monitoring individual's reliability and RUL, Eq.(41) and Eq.(42).

7. Simulation study

Numerical experiment is performed to demonstrate the

flexibility of the proposed approach. The true degradation model is assumed to within the Gamma and IG process, where the related mean functions are assumed to be S-shaped. The true model is presented in Table 1.

Table 1 The true model.

Candidate model	Model probability	Mean function	Model parameters
Gamma process model	0.5	$\Lambda_{Ga}(t) = \mu_{Ga} \exp(0.05(\alpha_{Ga}t) - (\alpha_{Ga}t)^{-1})$	$\begin{cases} \mu_{Ga} \sim f_N(2, 0.1) \\ \alpha_{Ga} \sim f_N(0.5, 0.05) \\ \lambda_{Ga} \sim f_N(0.1, 0.01) \end{cases}$
IG process model	0.5	$\Lambda_{IG}(t) = \mu_{IG} \exp(0.05(\alpha_{IG}t) - (\alpha_{IG}t)^{-1})$	$\begin{cases} \mu_{IG} \sim f_N(2, 0.1) \\ \alpha_{IG} \sim f_N(0.5, 0.05) \\ \lambda_{IG} \sim f_N(10, 1) \end{cases}$

Table 2. shows the process parameters are generated from the above true model. The proposed method's superiority on population evaluation is verified based on the first five samples. The proposed method's superiority on individual prediction is verified by using Sample 6.

Table 2 The model parameters randomly generated by true model.

Sample number	μ_{Ga}	α_{Ga}	λ_{Ga}	μ_{IG}	α_{IG}	λ_{IG}
1	1.9316	0.5143	0.0975	1.9863	0.4437	9.3435
2	1.9761	0.5012	0.0825	2.1417	0.5365	9.4746
3	1.8210	0.4793	0.1003	2.1076	0.4356	10.3692
4	2.0215	0.4208	0.0960	2.0633	0.5646	8.8680
5	2.0989	0.5267	0.0895	2.0375	0.5350	9.3218
6	2.0250	0.4751	0.0976	2.0589	0.5403	11.3934

Table 3. shows the six randomly generated samples, on the basis of the generated model parameters and the true degradation model. time increment $\Delta t=2$. The degradation mean is generally not complicated, so there are three hidden neurons in the presented simulation study. Referring to the degradation data of the first five degradation samples, the ANN supported Gamma and IG process models are trained by Eq.(21) and Eq.(24), respectively. The training results of the ANNs for the above two mentioned models are displayed in Table 4. For each sample, the model parameters' training results are displayed in Table 5. It should be noted that the randomly generated degradation dataset is non-dimensional, because above numerically generated degradation process has no real physical meaning.

Table 3 Generated degradation data.

Sample 1	1.4877	1.6396	1.8856	1.9731	2.0047	2.0988	2.1772	2.3276	2.6215
	2.7977	2.8215	2.9249	3.1968	3.4250	3.8054	3.8543	4.3150	4.5271
	4.6620	4.8670	5.0989	5.3243	5.6701	6.0881	6.3715		
Sample 2	1.5618	1.9479	2.0606	2.1684	2.3598	2.5238	2.5992	2.6793	2.8768
	3.0295	3.1585	3.3523	3.6713	3.8077	4.1519	4.3762	4.5029	4.7638
	4.9710	5.2241	5.3960	5.6910	5.9533	6.6217	7.0312		
Sample 3	1.8632	2.2946	2.4496	2.5801	2.6991	2.7535	2.8212	2.9726	3.0020
	3.0798	3.1517	3.1987	3.5806	3.6879	4.0069	4.1883	4.3054	4.6784
	4.8750	5.0790	5.2796	5.6850	5.9254	6.0798	6.2610		
Sample 4	1.8869	2.0946	2.3551	2.7385	2.9479	3.0687	3.1438	3.4180	3.5190
	3.5989	3.7181	3.7932	3.9430	4.0896	4.1576	4.4200	4.6958	4.7993
	4.9617	5.2170	5.4549	5.8435	6.4385	6.8768	7.1055		
Sample 5	1.6656	2.0201	2.1540	2.2174	2.4391	2.6000	2.6861	2.7672	2.9759
	3.2450	3.4791	3.7957	3.9916	4.1882	4.5071	4.6292	4.8034	4.9622
	5.3575	5.6821	6.1715	6.6432	6.8317	7.2832	7.7977		
Sample 6	1.4076	1.8481	1.9966	2.1234	2.2097	2.4271	2.4843	2.5436	2.7624
	3.0464	3.3173	3.6679	3.7653	4.1564	4.4175	4.8832	5.1580	5.4341
	5.6018	5.9013	6.1226	6.3647	6.6801	6.9203	7.1411		

Table 4 The training results of the ANN under Gamma and IG process models.

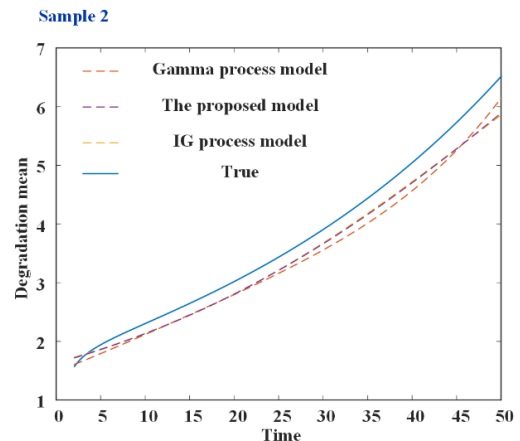
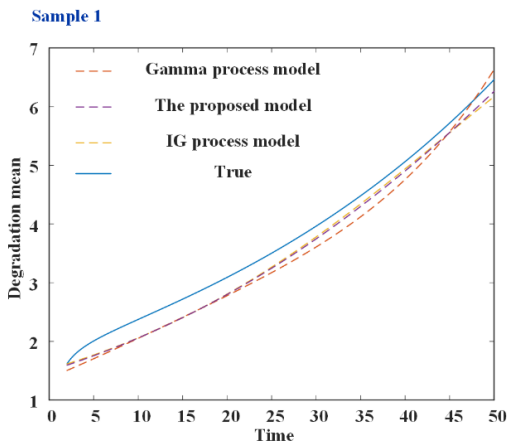
		$i=1$	$i=2$	$i=3$
Gamma process model	v_i	1.8812	2.1011	1.4701
	w_i	2.9552	0.0804	2.2935
	b_i	7.4186	0.2708	6.1968
IG process model	v_i	0.5835	0.1038	1.6922
	w_i	0.2043	0.0474	0.9063
	b_i	1.0148	0.2733	2.3237

The comparison of the true degradation mean curves and the

predicting mean curves of the different samples by the candidate models are displayed in Fig. 4. It is worth noting that the comparison Gamma process model and IG process model are also combined with ANN in this simulation study. The root mean squared errors (RMSEs) is used to reflect and compare the fitting accuracy of the candidate models. As indicated in Table 6, the proposed model is the best one considering the overall fitting accuracy.

Table 5 The training results of the ANN under Gamma and IG process models.

		Sample 1	Sample 2	Sample 3	Sample 4	Sample 5
Gamma process model	α_i	1.8263	1.7449	1.5272	1.5450	1.8356
	μ_i	4.2808	4.9081	5.5445	5.8413	5.0825
	λ_i	0.1011	0.0551	0.1688	0.1693	0.0603
IG process model	α_i	1.5290	1.4303	1.1689	1.1787	1.5512
	μ_i	1.2545	1.4519	1.6792	1.8016	1.4796
	λ_i	0.7631	0.7557	0.7490	0.7092	0.7532
	ρ_{ai}	0.1919	0.1093	0.3998	0.3813	0.1106



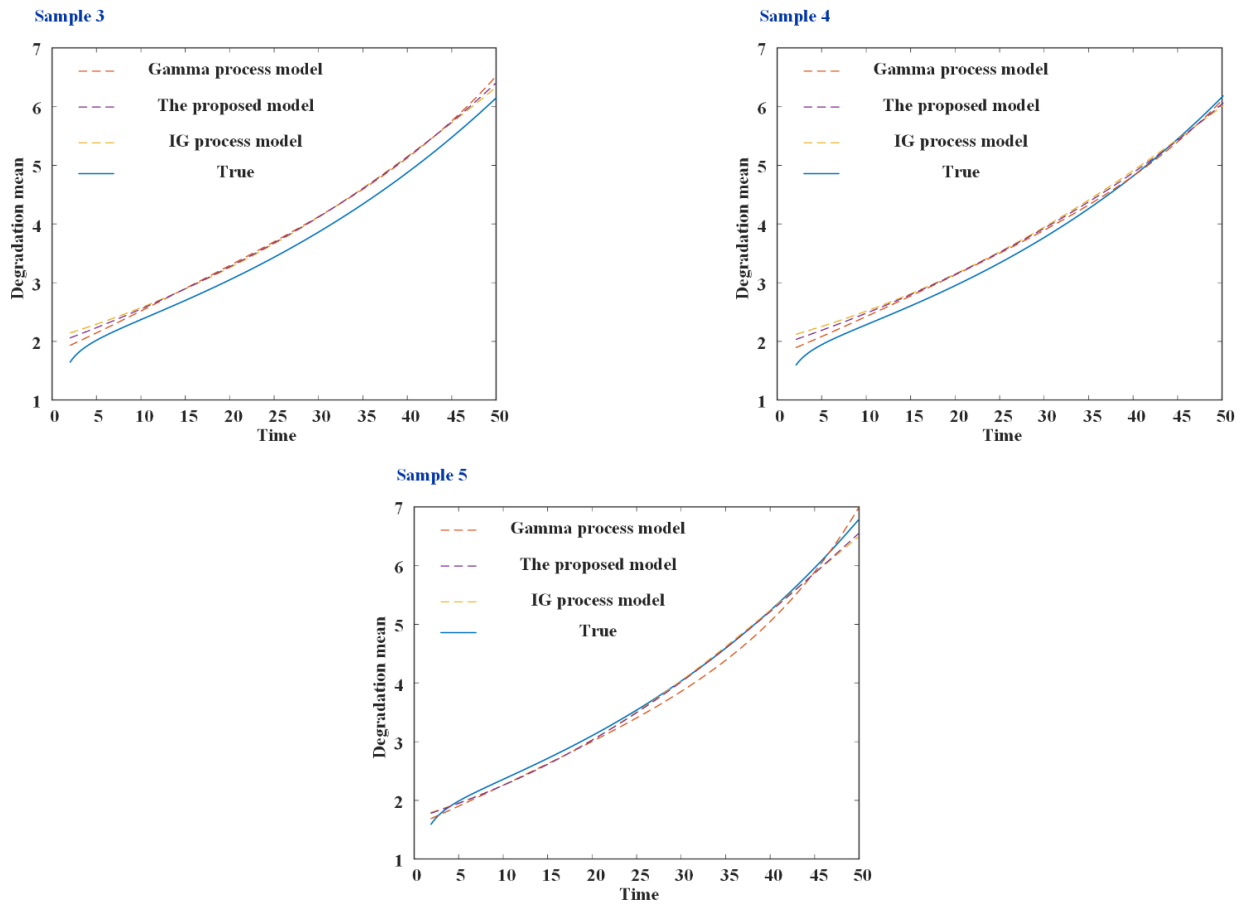


Fig. 4. Comparisons of the true degradation mean and the predictions for the individuals.

Table 6 RMSEs of mean function of the Gamma, IG and proposed models.

	Gamma process model	IG process model	The proposed model
Sample 1	0.2973	0.2309	0.2389
Sample 2	0.3832	0.3337	0.3374
Sample 3	0.2454	0.2593	0.2511
Sample 4	0.1658	0.2516	0.2169
Sample 5	0.1602	0.1141	0.1075
Average	0.2504	0.2379	0.2303

The hyper-parameters of each candidate distributions are evaluated by employing the model parameters' training results and ME method, Eq.(29) and Eq.(30). AIC method is utilized to measure the goodness-of-fit of the candidate distributions. The ME estimating results and the corresponding AIC values are displayed in Table 7. The distributions with the minimum AIC values are selected, as Eq.(43) and Eq.(44).

Table 7 The ME results and corresponding AIC values of different distributions.

		Gamma			lognormal			Gaussian		
		δ	γ	AIC	δ	γ	AIC	δ	γ	AIC
Gamma process model	α	159.4905	0.0106	-1.8270	0.5250	0.0802	-1.7909	1.6958	0.1343	-1.8890
	μ	90.7759	0.0565	12.0992	1.6297	0.1073	12.1632	5.1314	0.5386	12.0013
	λ	4.9082	0.0226	-12.2176	-2.3109	0.4820	-12.2168	0.1109	0.0501	-11.7563
IG process model	α	67.7944	0.0202	0.3495	0.3084	0.1241	0.4029	1.3716	0.1666	0.2669
	μ	65.1250	0.0235	1.5884	0.4197	0.1253	1.6148	1.5334	0.1900	1.5825
	λ	1544.9121	0.000483	-21.3435	-0.2933	0.0259	-21.2893	0.7460	0.0190	-21.4541
	p_{Ga}	3.4856	0.0684	-3.2574	-1.5895	0.5679	-3.3643	0.2386	0.1278	-2.3842

$$\left\{ \begin{aligned} \alpha_{Ga} &\sim f_N(1.6958, 0.1343), \mu_{Ga} \sim f_N(5.1314, 0.5386) \\ \lambda_{Ga} &\sim f_{Ga}(4.9082, 0.0226), p_{Ga} \sim f_{LN}(-1.5895, 0.5679) \end{aligned} \right. \quad (43)$$

$$\left\{ \begin{aligned} \alpha_{IG} &\sim f_N(1.3716, 0.1666), \mu_{IG} \sim f_N(1.5334, 0.1900) \\ \lambda_{IG} &\sim f_N(0.7460, 0.0190), p_{IG} = 1 - p_{Ga} \end{aligned} \right. \quad (44)$$

The comparison of the true degradation mean curve and the predicting mean curve of the population by the candidate models are shown in Fig. 5. The RMSEs is used to reflect and

compare the fitting accuracy of the candidate models. As indicated in Table 6 the proposed model is the best one considering the overall fitting accuracy.

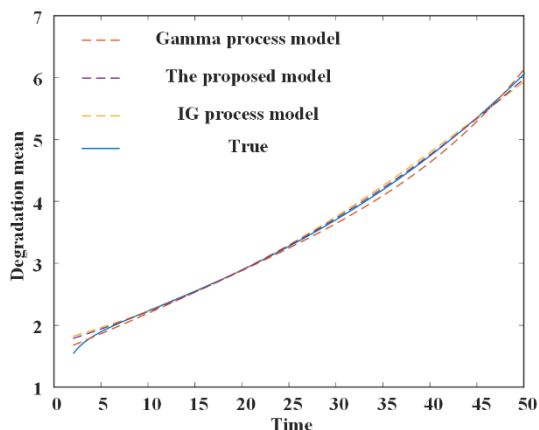


Fig. 5. Comparisons of the true degradation mean and the predictions for the population.

Table 8 RMSEs of mean function of the Gamma, IG and proposed models.

	Gamma process model	IG process model	The proposed model
RMSE	0.0803	0.0936	<u>0.0757</u>

According to the above estimated distributions of the model probabilities and parameters, the life distribution and reliability curve are calculated by Eq.(33) and Eq.(34), respectively. Fig. 6 shows the comparison of the population life distribution and the corresponding predictions given by the candidate models. Fig. 7 shows the comparisons of the true population reliability curve and the corresponding predictions given by the candidate models. The proposed model guarantees the highest accuracies on population life distribution and population reliability curve predictions among the candidate models.

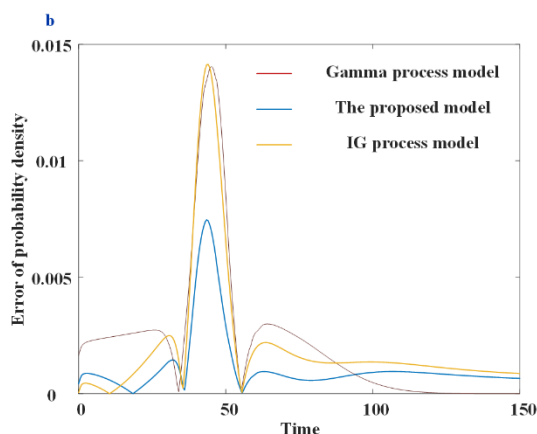
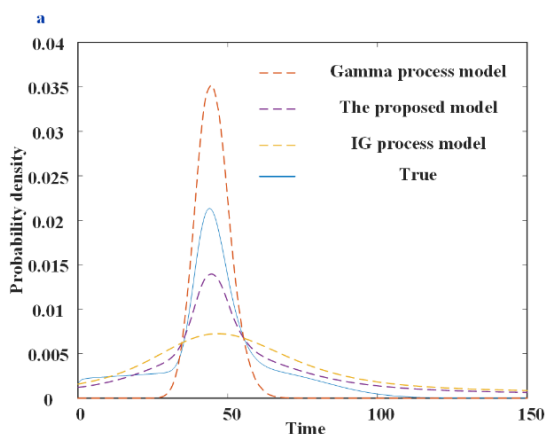


Fig. 6. Comparisons of the population life distribution and the related predictions.

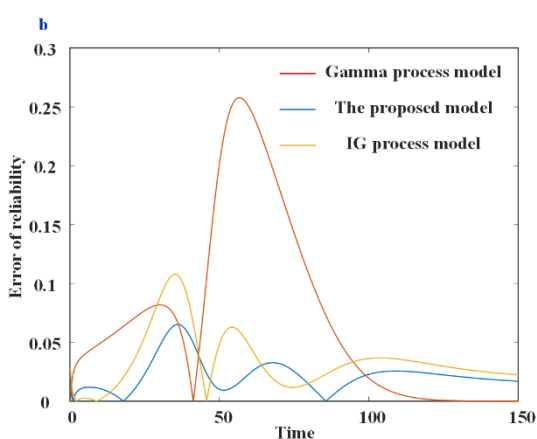
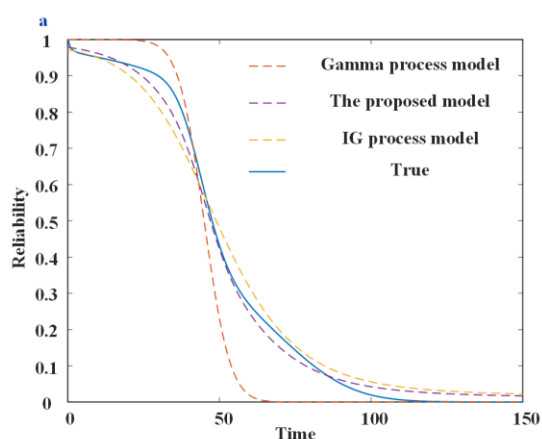


Fig. 7. Comparisons of the population reliability curve and the related predictions.

The estimations of the model parameters for sample 6 are displayed in Table 9. The comparison of the true degradation mean and the predicting mean curve of sample 6 by the candidate models are shown in Fig. 8. The RMSEs is used to

reflect and compare the fitting accuracy of the candidate models. As indicated in Table 10, the proposed model is the best one considering the overall fitting accuracy.

Table 9 Estimated model parameters for sample 6.

	α_{Ga}	μ_{Ga}	λ_{Ga}	p_{Ga}	α_{IG}	μ_{IG}	λ_{IG}
Sample 6	1.699	5.131	0.11	0.1789	1.37	1.538	0.7193

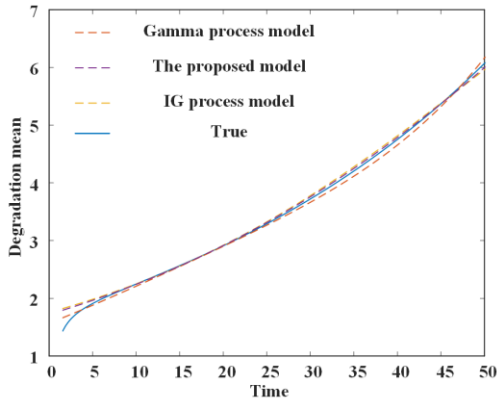


Fig. 8. Comparisons of the true degradation mean and the related predictions.

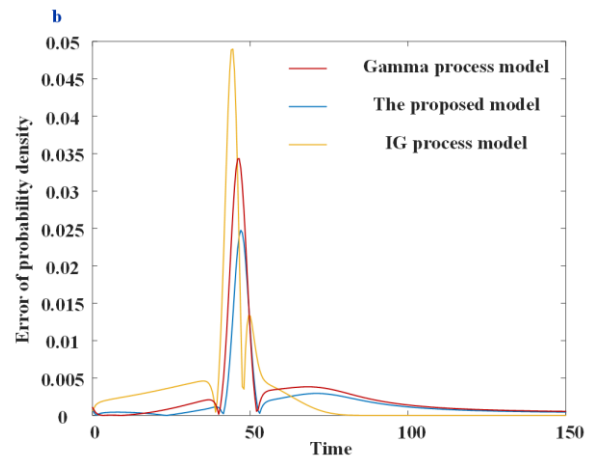
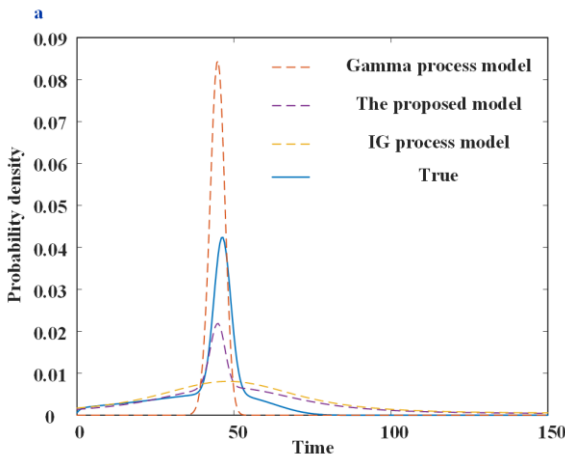


Fig. 9. Comparisons of the individual life distribution and the related predictions.

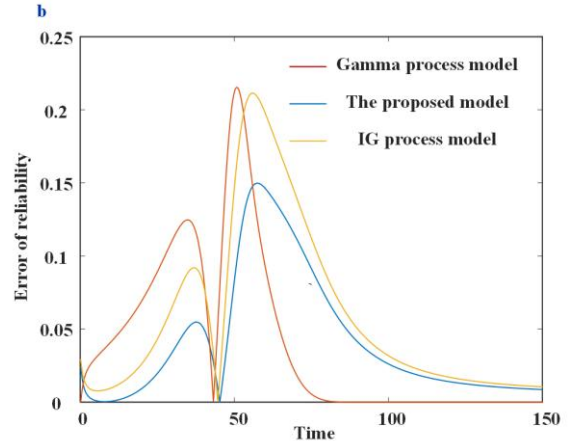
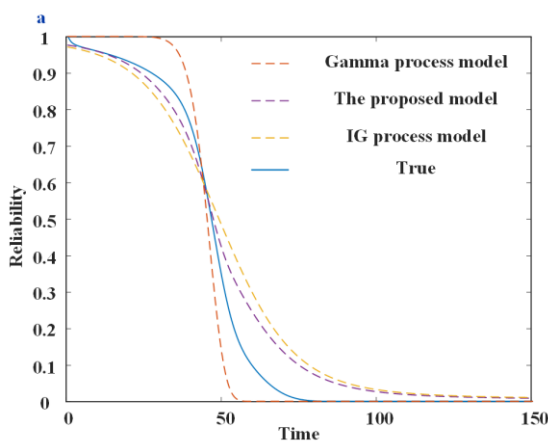


Fig. 10. Comparisons of the individual reliability curve and the related predictions.

8. Case study

In order to substantiate the effectiveness of the proposed method, an actual degradation dataset related to spindle system's machining accuracy is applied, which is presented in Ref. 26.

Table 10 RMSEs of mean function of the Gamma, IG and proposed models.

	Gamma process model	IGprocess model	The proposed model
RMSE	0.0674	0.0792	<u>0.0625</u>

Fig. 9 shows the comparison of the life distribution of sample 6 and the corresponding predictions given by the candidate models. Fig. 10 shows the comparison of the true reliability curve of sample 6 and the corresponding predictions given by the candidate models. The proposed model maintains the highest accuracies on individual life distribution and reliability curve predictions among the candidate models.

Machining accuracy of five spindle systems using for production is monitored. The machining accuracy is measured discretely during spare time of the machine tools. The degradation dataset is shown in Fig 11.

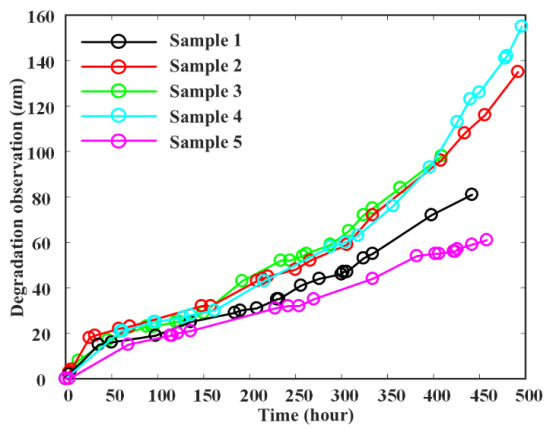


Fig. 11. Field data of machining accuracy.

Table 11. The training results of the ANN under Gamma and IG process models.

		$i=1$	$i=2$	$i=3$
Gamma process model	v_i	1.3434	-9.9996	1.2090
	w_i	2.0395	-4.5451	8.9770
	b_i	4.8778	5.0080	6.3195
IG process model	v_i	-1.9463	0.5431	1.3998
	w_i	-0.4673	1.2425	1.7647
	b_i	1.6244	2.7714	4.3418

Table 12 The training results of the ANN under Gamma and IG process models.

		Sample 1	Sample 2	Sample 3	Sample 4	Sample 5
Gamma process model	α_i	1.8224	2.1856	1.7966	1.8460	2.0930
	μ_i	3.2221	3.1263	2.4189	3.0940	1.8276
	λ_i	0.1389	0.1950	0.0763	0.1105	0.0480
IG process model	α_i	1.9009	1.9701	1.7891	1.7063	1.5149
	μ_i	1.8412	1.7755	1.4899	1.9523	1.1215
	λ_i	0.6543	0.5226	0.5861	0.6003	0.6311
	p_{ai}	0.4918	0.4780	0.5695	0.5859	0.4746

Referring to the training results, the degradation mean curves of each samples can be calculated by Eq.(4). The RMSEs of the degradation modeling of the Gamma, IG, the proposed models and the method presented in Ref. 30 are indicated in Table 13. It should be mentioned that the comparison models

Table 13 RMSEs of degradation modeling of the Gamma, IG and proposed models.

	Gamma process model	IG process model	The proposed model	The method presented in Ref. [30]
Sample 1	2.6379	8.6230	2.0143	15.2737
Sample 2	33.4914	16.5695	16.5734	4.1135
Sample 3	2.4420	2.6063	1.8884	6.5882
Sample 4	2.5404	4.1643	7.6094	12.3729
Sample 5	17.9597	2.2261	5.4903	3.2624
Average	11.8143	6.8378	6.7152	8.3221

The hyper-parameters of each candidate distributions are evaluated by using the model parameters' training results and ME method, Eq.(29) and Eq.(30). AIC method is employed to evaluate the goodness-of-fit of the candidate distributions.

The degradation mean is generally not complicated, so there are three hidden neurons in the presented case study. According to the degradation data of all the five degradation samples, the ANN supported Gamma and IG process models are trained by Eq.(21) and Eq.(24), respectively. The training results of the ANNs for the above two mentioned models are displayed in Table 11. For each sample, the model parameters' training results are displayed in Table 12. The model probabilities for each samples can be evaluated by Bayesian inference method are shown in Eq.(25) and are displayed in Table 12.

are also means the ANN supported Gamma and IG process models. Evidently, the proposed model can provide the highest accuracy on the degradation mean prediction among the candidate methods.

displays the ME estimating results and the corresponding AIC values. The distributions with the minimum AIC values are selected, as Eq.(45) and Eq.(46).

Table 14 The ME results and corresponding AIC values of different distributions.

		Gamma			lognormal			Gaussian		
		δ	γ	AIC	δ	γ	AIC	δ	γ	AIC
Gamma process model	α	149.9907	0.0130	-0.3276	0.6639	0.0803	-0.3912	1.9487	0.1591	-0.1918
	μ	25.9782	0.1054	12.5060	0.9851	0.2170	12.7606	2.7378	0.5371	11.9746
	λ	4.9855	0.0228	12.0145	-2.2844	0.4847	11.8964	0.1137	0.0509	11.5833
IG process model	α	124.7252	0.0142	-0.0549	0.5704	0.0919	0.0239	1.7763	0.1590	-0.1961
	μ	29.8948	0.0547	6.6210	0.4734	0.2007	6.8651	1.6361	0.2992	6.1240
	λ	177.7302	0.0034	-12.6971	-0.5156	0.0769	-12.6208	0.5989	0.0449	-12.8391
	p_{Ga}	118.4385	0.0044	-12.3545	-0.6581	0.0905	-12.4145	0.5200	0.0478	-12.2226

$$\begin{cases} \alpha_{Ga} \sim f_{LN}(0.6639, 0.0803), \mu_{Ga} \sim f_N(2.7378, 0.5371) \\ \lambda_{Ga} \sim f_N(0.1137, 0.0509), p_{IG} \sim f_{LN}(-0.6581, 0.0905) \end{cases} \quad (45)$$

$$\begin{cases} \alpha_{IG} \sim f_N(1.7763, 0.1590), \mu_{IG} \sim f_N(1.6361, 0.2992) \\ \lambda_{IG} \sim f_N(0.5989, 0.0449), p_{IG} = 1 - p_{Ga} \end{cases} \quad (46)$$

Referring to the above estimated distributions of the model probabilities and parameters, the life distribution and reliability curve can be calculated by Eq.(33) and Eq.(34), respectively. They are compared to the life distributions and reliability curves calculated by the corresponding Gamma and IG process models. According to Fig. 12 and Fig 13, the process uncertainty issues should be considered when analyzing the population life distribution and reliability, considering the highest accuracy of the proposed model among the candidate models and the differences of life distributions and reliability curves.

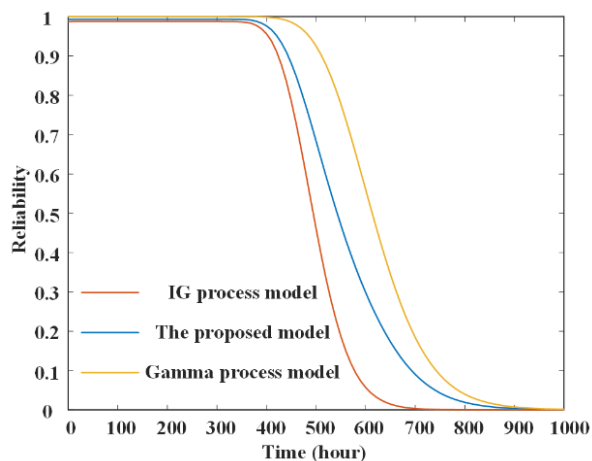


Fig. 12. The population reliability curves given by Gamma process model, IG process model and the proposed model.

To evaluate the effectiveness of the proposed approach on individual reliability prediction, another four samples are employed to estimate the superiority of the model probabilities and parameters when one specific sample is used as the monitoring individual.

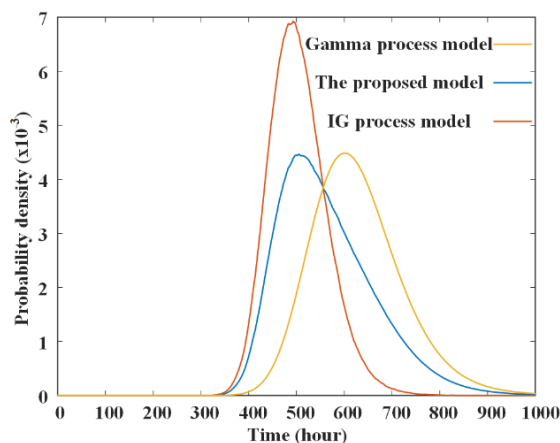


Fig. 13. The population life distributions given by Gamma process model, IG process model and the proposed model.

For example, sample 1 to sample 4 are used to evaluate the priors, when sample 5 is used as the monitoring individual. Furthermore, the last three observations are retained for cross validations. Namely, the first sixteen observations are used to infer the model parameters and probabilities.

Table 15 Estimated model parameters for different degradation samples.

	α_{Ga}	μ_{Ga}	λ_{Ga}	p_{Ga}	α_{IG}	μ_{IG}	λ_{IG}
Sample 1	1.8354	3.1918	0.1456	0.5185	1.8614	1.8963	0.6246
Sample 2	1.6330	3.6313	0.1743	0.5077	1.8867	1.8631	0.6120
Sample 3	1.6139	2.8191	0.1070	0.5499	1.7696	1.5287	0.6182
Sample 4	1.8524	3.0776	0.1294	0.5632	2.0071	1.8179	0.6157
Sample 5	1.3703	2.7021	0.0870	0.5164	1.6348	1.3565	0.6218

Table 15 shows the estimated model parameters of the proposed model. The boxplots of the degradation predictions given by the proposed model are shown in Fig. 14. To quantitatively analyze the accuracy of the proposed model, the RMSEs of the Gamma process model, IG process model, the method presented in Ref. 32 and proposed model are calculated and displayed Table 16, Intuitively, when focusing on the degradation predicting accuracy, the proposed model is the best one.

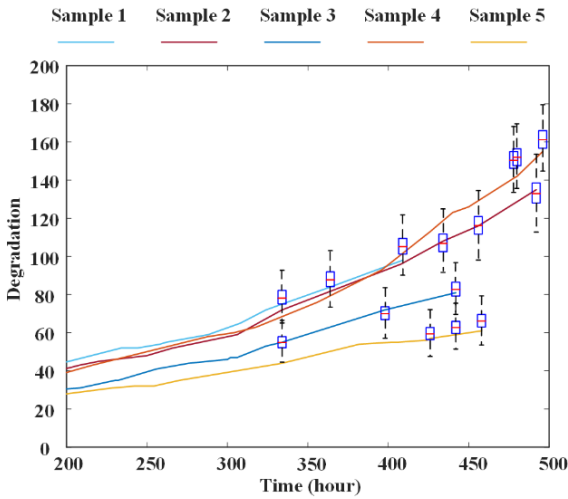


Fig. 14. The degradation predictions given by the proposed model.

Furthermore, the proposed model has also been compared to several previous published models for validating its effectiveness. The model presented in Ref. [30] neglects process uncertainty and random effects. The model presented in Ref. [40] neglects process uncertainty. The model presented in Ref. [26] neglects mean function uncertainty. Consistent with the above mentioned researches, the relative error is defined by Eq.(47). The prediction mean squared errors (MSEs) of the degradation prediction relative error for the different candidate models are shown in Table 17. Obviously, the proposed model is more effective than the other candidate models focusing on the degradation predicting accuracy, due to considering the multi-uncertainties simultaneously.

$$error = \frac{|\text{inferred degradation} - \text{observed degradation}|}{\text{observed degradation}} \quad (47)$$

Table 16 RMSEs of the degradation predictions for different degradation samples.

	Gamma process model	IG process model	The proposed model	The method presented in Ref. [30]
Sample 1	1.5837	2.1592	0.6839	1.1125
Sample 2	0.9054	3.6708	0.6212	1.2442
Sample 3	0.8361	0.5493	0.5753	1.2713
Sample 4	0.7802	1.4264	1.8092	0.7275
Sample 5	1.1801	0.4924	1.6443	1.8425
Average	1.2365	1.6596	1.0668	1.2396

Table 17 MSEs of the degradation predictions of the candidate methods.

Method	The proposed model	The previous model in Ref.[30]	The previous model in Ref.[40]	The model presented in Ref.[26]
MSE	0.401x10 ⁻³	0.455x10 ⁻³	2.836x10 ⁻³	2.265x10 ⁻³

Fig. 15 and Fig. 16 show the individual RUL distributions and reliability curves of each monitoring individuals given by the proposed method, respectively.

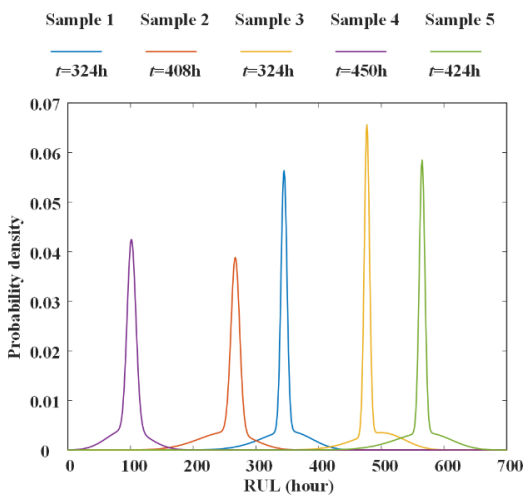


Fig. 15. The individual RUL distributions of different degradation samples given by the presented method.

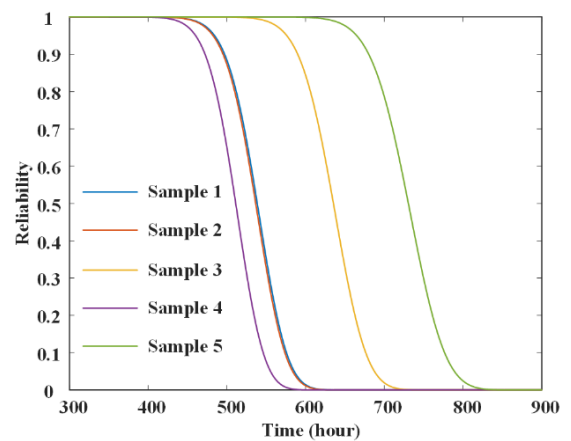


Fig. 16. The individual reliability curves of different degradation samples given by the presented method.

9. Conclusions

This paper presents an ANN-supported stochastic process for reliability analysis with the mean function uncertainty, random

effects and process uncertainty simultaneously. The ANN supported Gamma and IG process models with random effects are constructed and used as the candidate models. The corresponding parameters and model probabilities estimation method is also built based on ME, AIC and fully Bayesian inference methods, such that the proposed stochastic processes can be applied to population degradation model and monitor individual degradation prediction.

Simulation experiment is performed to demonstrate the flexibility of the proposed method. The simulation results indicate that the proposed model provides the highest accuracies on life distribution and reliability curve predictions among the candidate models. Furthermore, a degradation experimental

dataset about the machining accuracy is also applied to substantiate the performance of the proposed method. The proposed method maintains superiorities on the population reliability analysis and monitoring individual reliability prediction focusing on the degradation modeling and predicting accuracies. Furthermore, it can also give the reliability curves and life (or RUL) distributions of the monitoring individual and evaluating population. Namely, the propose method is more workable for some actual applications, especially for analyzing the monotonous degradation dataset.

Further work will focus on handling the multi uncertainty issues in accelerating degradation test and accelerated life test planning.

Acknowledgements

This study was co-supported by the National Natural Science Foundation of China (52105045, 52475046), the Aviation Science Foundation (2022Z027051001), Ningbo Key R&D Program (2023Z010), Beijing Natural Science Foundation (L221008) and the Foundation of Tianmushan Laboratory (TK-2023-C-006).

References

1. Ma ZH, Nie SL, Liao HT. A load spectra design method for multi-stress accelerated testing. *Journal of Risk and Reliability* 2022; 236(6): 994-1006. <https://doi.org/10.1177/1748006X211062012>.
2. He R, Chen GM, Shen XY, et al. Reliability assessment of repairable closed-loop process systems under uncertainties. *ISA Transactions* 2020; 104: 222-232. <https://doi.org/10.1016/j.isatra.2020.05.008>.
3. Li ZL, Zheng ZX and Rachid O. A prognostic methodology for power MOSFETs under thermal stress using echo state network and particle filter. *Microelectronics Reliability* 2018; 88: 350-354. <https://doi.org/10.1016/j.microrel.2018.07.137>.
4. Ma R, Yang T, Breaz E, et al. Data-driven proton exchange membrane fuel cell degradation predication through deep learning method. *Applied Energy* 2018; 231: 102-115. <https://doi.org/10.1016/j.apenergy.2018.09.111>.
5. Chen X, Liu Z, Wang J, et al. An adaptive prediction model for the remaining life of an Li-ion battery based on the fusion of the two-phase wiener process and an extreme learning machine. *Electronics* 2021; 10: 540. <https://doi.org/10.3390/electronics10050540>.
6. Hong W, Wang SP, Tomovic MM, et al. A novel indicator for mechanical failure and life prediction based on debris monitoring. *IEEE Trans Reliab* 2016; 66: 161-169. <https://doi.org/10.1109/TR.2016.2628412>.
7. Nie SL, Song YX, Ma ZH, Yin FL, Ji H. Reliability assessment of PEEK/17-4PH stainless steel tribopair under seawater lubrication. *Journal of Risk and Reliability* 2023; 237(1): 29-39. <https://doi.org/10.1177/1748006X221086915>.
8. Yang CY, Ma J, Wang XD, et al. A novel based-performance degradation indicator 456 RUL prediction model and its application in rolling bearing. *ISA Transactions* 2021; 121: 349-364. <https://doi.org/10.1016/j.isatra.2021.03.045>.
9. Wang X. Wiener processes with random effects for degradation data. *Journal of Multivariate Analysis* 2010; 101: 340-351. <https://doi.org/10.1016/j.jmva.2008.12.007>.
10. Pan DH, Wei YT, Fang HZ, et al. A reliability estimation approach via Wiener degradation model with measurement errors. *Applied Mathematics and Computation* 2018; 320: 131-141. <https://doi.org/10.1016/j.amc.2017.09.020>.
11. Dong QL, Cui LR and Si SB. Reliability and availability analysis of stochastic degradation systems based on bivariate wiener processes. *Applied Mathematical Modelling* 2019; 79: 414-433. <https://doi.org/10.1016/j.apm.2019.10.044>.
12. Park C and Padgett WJ. Accelerated degradation models for failure based on geometric Brownian motion and gamma processes. *Lifetime Data Analysis* 2005; 11: 511-527. <https://doi.org/10.1007/s10985-005-5237-8>.
13. Ye ZS and Chen N. The inverse Gaussian process as a degradation model. *Technometrics* 2014; 56: 302-311.

<https://doi.org/10.1080/00401706.2013.830074>.

14. Ye ZS, Chen LP, Tang LC, et al. Accelerated degradation test planning using the inverse gaussian process. *IEEE Transactions on Reliability* 2014; 63: 750-763. <https://doi.org/10.1109/TR.2014.2315773>.
15. Peng CY. Inverse Gaussian processes with random effects and explanatory variables for degradation data. *Technometrics* 2015; 57: 100-111. <https://doi.org/10.1080/00401706.2013.879077>.
16. Jiang PH, Wang BX, Wang XF, et al. Inverse Gaussian process based reliability analysis for constant-stress accelerated degradation data. *Applied Mathematical Modelling* 2022; 105: 137-148. <https://doi.org/10.1016/j.apm.2021.12.003>.
17. Tseng ST, Balakrishnan N and Tsai CC. Optimal step-stress accelerated degradation test plan for gamma degradation processes. *IEEE Transactions on Reliability* 2009; 58: 611-618. <https://doi.org/10.1109/TR.2009.2033734>.
18. Wu B, Cui LR and Yin J. Reliability and maintenance of systems subject to Gamma degradation and shocks in dynamic environments. *Applied Mathematical Modelling* 2021; 96: 367-381. <https://doi.org/10.1016/j.apm.2021.03.009>.
19. Park C and Padgett WJ. Stochastic degradation models with several accelerating variables. *IEEE Trans Rel* 2006; 55: 379-390. <https://doi.org/10.1109/TR.2006.874937>.
20. Sugiura N. Further analysis of the data by Akaike's information criterion and the finite corrections. *Commun Stat Theory Methods* 1978; 7: 13-26. <https://doi.org/10.1080/03610927808827599>.
21. Hurvich CM and Tsai CL. Regression and time series model selection in small samples. *Biometrika* 1989; 76: 297-307. <https://doi.org/10.1093/biomet/76.2.297>.
22. Liu L, Li XY, Zio E, et al. Model uncertainty in accelerated degradation testing analysis. *IEEE Trans Reliab* 2017; 99: 1-13. <https://doi.org/10.1109/TR.2017.2696341>.
23. Liu D, Wang SP, Zhang C, et al. Bayesian model averaging based reliability analysis method for monotonic degradation dataset based on inverse Gaussian process and Gamma process. *Reliability Engineering & System Safety* 2018; 180: 25-38. <https://doi.org/10.1016/j.ress.2018.06.019>.
24. Liu D, Wang SP and Tomovic MM. Degradation modeling method for rotary lip seal based on failure mechanism analysis and stochastic process. *Eksploatacja i Niezawodność-Maintenance and Reliability* 2020; 22: 381-390. DOI: <https://doi.org/10.17531/ein.2020.3.1>.
25. Peng WW, Li YF, Yang YJ, et al. Leveraging Degradation testing and condition monitoring for field reliability analysis with time-varying operating missions. *IEEE Transactions on Reliability* 2015; 64: 1367-1382. <https://doi.org/10.1109/TR.2015.2443858>.
26. Peng WW, Li YF, Yang YJ, et al. Bayesian degradation analysis with inverse gaussian process models under time-varying degradation rates. *IEEE Transactions on Reliability* 2017; 66: 84-96. <https://doi.org/10.1109/TR.2016.2635149>.
27. Liu K, Zou TJ, Dang W, et al. Misspecification analysis of two phase gamma liner degradation models. *Quality and Reliability Engineering International* 2020; 36: 2066-2084. <https://doi.org/10.1002/qre.2674>.
28. Kong D, Balakrishnan N and Cui LR. Two-phase degradation process model with abrupt jump at change point governed by Wiener process. *IEEE Trans Reliab* 2017; 66: 1345-1360. <https://doi.org/10.1109/TR.2017.2711621>.
29. Zhang JX, Si XS, Du DB, et al. Lifetime estimation for multi-phase deteriorating process with random abrupt jumps. *Sensors* 2019; 19: 1472. <https://doi.org/10.3390/s19061472>.
30. Liu D, Wang SP and Cui XY. An artificial neural network supported Wiener process based reliability estimation method considering individual difference and measurement error. *Reliability Engineering & System Safety* 2021; 218: 108162. <https://doi.org/10.1016/j.ress.2021.108162>.
31. Peng CY. Inverse Gaussian processes with random effects and explanatory variables for degradation data. *Technometrics* 2015; 57: 100-111. <https://doi.org/10.1080/00401706.2013.879077>.
32. Rodríguez-Picón LA, Rodríguez-Picón AP, Méndez-González LC, et al. Degradation modeling based on gamma process models with random effects. *Commun Stat-Simul Comput* 2018; 47: 1796-1810. <https://doi.org/10.1080/03610918.2017.1324981>.
33. Li XY, Wu JP, Ma HG, et al. A random fuzzy accelerated degradation model and statistical analysis. *IEEE Transactions on Fuzzy Systems* 2018; 26: 1638-1650. <https://doi.org/10.1109/TFUZZ.2017.2738607>.
34. Liu D and Wang SP. A degradation modeling and reliability estimation method based on Wiener process and evidential variable. *Reliability Engineering & System Safety* 2020; 202: 106957. <https://doi.org/10.1016/j.ress.2020.106957>.

35. Peng WW, Huang HZ, Xie M, et al. A Bayesian approach for system reliability analysis with multilevel pass-fail, lifetime and degradation data sets. *IEEE Transactions on Reliability* 2013; 62: 689-699. <https://doi.org/10.1109/TR.2013.2270424>.
36. Peng WW, Li YF, Yang YJ, et al. Inverse Gaussian process models for degradation analysis: a Bayesian perspective. *Reliab Eng Syst Saf* 2014; 13: 175-89. <https://doi.org/10.1016/j.res.2014.06.005>.
37. Guan Q, Tang YC and Xu AC. Objective Bayesian analysis accelerated degradation test based on Wiener process models. *Applied Mathematical Modelling* 2016; 40: 2743-55. <https://doi.org/10.1016/j.apm.2015.09.076>.
38. Jia X. Reliability analysis for Weibull distribution with homogeneous heavily censored data based on Bayesian and least-squares methods. *Applied Mathematical Modelling* 2020; 83: 169-188. <https://doi.org/10.1016/j.apm.2020.02.013>.
39. Guo JY, Li YF, Peng WW, et al. Bayesian information fusion method for reliability analysis with failure-time data and degradation data. *Quality and Reliability Engineering International* 2022; 38: 1944-1956. <https://doi.org/10.1002/qre.3065>.
40. Liu D, Wang SP. An artificial neural network supported stochastic process for degradation modeling and prediction. *Reliability Engineering & System Safety* 2021; 214 (5):107738. <https://doi.org/10.1016/j.res.2021.107738>.